



Atlas for the Lateralized Visuospatial Attention Networks (ALANs): Insights from fMRI and network analyses

Loïc Labache^{a,b,c}, Laurent Petit^b, Marc Joliot^b, Laure Zago^b

^aDepartment of Psychology, Yale University, New Haven, CT, United States

^bUniv. Bordeaux, CNRS, CEA, IMN, UMR, 5293, Bordeaux, France

^cDepartment of Psychiatry, Brain Health Institute, Rutgers University, Piscataway, NJ, United States

Corresponding Authors: Loïc Labache (loic.labache@yale.edu); Laure Zago (laure.zago@u-bordeaux.fr)

ABSTRACT

Hemispheric specialization is central to human evolution and fundamental to human cognitive abilities. While being a defining feature of functional brain architecture, hemispheric specialization is overlooked to derive brain parcellations. Alongside language, which is typically lateralized in the left hemisphere, visuospatial attention is set to be its counterpart in the opposite hemisphere. However, it remains uncertain to what extent the anatomical and functional underpinnings of lateralized visuospatial attention mirror those supporting language. Building on our previous work, which established a lateralized brain atlas for language, we propose a comprehensive cerebral lateralized atlas delineating the anatomo-functional bases of visuospatial attention, Atlas for Lateralized visuospatial Attentional Networks (ALANs). Combining task and resting-state functional connectivity analyses, we identified 95 lateralized brain areas comprising three networks supporting visual (visu), motor (somato-motor), and spatial processing (posterior-medial) processes at work during a line judgment bisection task, and two large-scale networks related to integrated visuospatial attention processes, the parieto-frontal and temporo-frontal networks. We identify hubs playing a pivotal role in the intra-hemispheric interaction within visuospatial attentional networks. The rightward lateralized parieto-frontal encompasses one hub, the inferior frontal sulcus, while the temporo-frontal network encompasses two right hubs: the inferior frontal cortex (*pars triangularis* and the anterior insula) and the posterior part of the superior temporal sulcus. Compared with our language lateralized atlas, we demonstrated that specific regions within these networks encompass the homotope of the language network from the left hemisphere. This atlas of visuospatial attention provides valuable insights for future investigations into the variability of visuospatial attention and hemispheric specialization research. Additionally, it facilitates more effective comparisons among different studies, thereby enhancing the robustness and reliability of research in the field of attention.

Keywords: visuospatial attention, right lateralization, intrinsic connectivity, hemispheric specialization, parieto-frontal network, temporo-frontal network

1. INTRODUCTION

Hemispheric specialization is a fundamental principle in the functional organization of the human brain (Hervé et al., 2013). In about 90% of humans, who are right-handers, the left hemisphere is specialized for language

and the motor control of their dominant hand (Labache et al., 2020, 2023; Mazoyer et al., 2014). In contrast, the right hemisphere is more dedicated to controlling visuospatial skills, including spatial attention (Hervé et al., 2013). This complementary hemispheric pattern between

Received: 14 February 2024 Revision: 3 May 2024 Accepted: 4 June 2024 Available Online: 11 June 2024



The MIT Press

© 2024 The Authors. Published under a Creative Commons Attribution 4.0 International (CC BY 4.0) license.

Imaging Neuroscience, Volume 2, 2024
https://doi.org/10.1162/imag_a_00208

the language and spatial domain most likely results from evolutionary adaptive processes and selection pressure (Güntürkün & Ocklenburg, 2017; Heger et al., 2020). A significant contributor to this development and maintenance of hemispheric asymmetry is probably the corpus callosum, as suggested by Gazzaniga (2000). However, the origin of the complementary patterns in hemispheric specialization is still a matter of debate (Francks, 2019; Gerrits, 2022; Thiebaut de Schotten et al., 2019; Tzourio-Mazoyer et al., 2020; Vingerhoets, 2019). Indeed, these complementary patterns remain misunderstood since they appear variable across the population, with a dependent relationship between language and spatial hemispheric lateralization only present in strongly left-handed individuals (Zago et al., 2016), while independence seems to be the rule for right-handed and mixed-handed individuals (Jia et al., 2021; Zago et al., 2016). This highlights the need to elaborate a normalized atlas to systematize the investigation of the lateralization of visuospatial processes at a regional level (Yeo & Eickhoff, 2016).

Although the identification of the neural attentional networks has been performed using various neuroimaging techniques in healthy individuals and patients with spatial neglect (Corbetta & Shulman, 2011; Petersen & Posner, 2012), the study of the lateralization has mainly been overlooked as compared to language (Hervé et al., 2013; Josse & Tzourio-Mazoyer, 2004; Mengotti et al., 2020; Tzourio et al., 1998). Visuospatial attention is a cognitive function traditionally lateralized to the right hemisphere (Heilman et al., 1993; Karnath & Rorden, 2012; Kinsbourne, 1970; Mesulam, 1999), as evidenced by the neuropsychological literature indicating spatial neglect after occipito-parietal lesions in the right hemisphere (Coppens et al., 2002; Dronkers & Knight, 1989; Suchan & Karnath, 2011). Unlike the lateralization of language, extensively studied and well defined through established gold standard paradigms and techniques to explore its anatomo-functional bases, visuospatial functions lack a similar approach (Hervé et al., 2013). We have previously demonstrated that the line bisection judgment task, an fMRI-adapted version of the line bisection task, is suitable for investigating both the asymmetry of brain regions involved in spatial attention and hemispheric lateralization in healthy participants (Zago et al., 2016; Zago, Petit, et al., 2017).

A complex network of brain regions supports visuospatial attention. Neuropsychological studies differentiate attentional processes into two distinct types (Petersen & Posner, 2012): a slow, goal-oriented, and voluntary aspect, contrasted with a rapid, involuntary, stimulus-driven, and automatic element. The first one, the dorsal attentional network, encodes and sustains preparatory

cues while modulating top-down sensory (visual, auditory, olfactory, and somatosensory) regions (Corbetta & Shulman, 2002). The second one, the ventral attentional network, activates when attention shifts to new, behaviorally significant events (Corbetta & Shulman, 2002). Key components of the dorsal network classically include the intraparietal sulcus, the superior parietal lobe, and the frontal eye fields at the junction between the superior frontal and precentral sulci. In contrast, the temporoparietal junction, the inferior part of the middle frontal gyrus, the inferior frontal gyrus, and the anterior insula constitute the core regions of the ventral network. In addition to these cortical structures, a set of subcortical structures, including the pulvinar, the superior colliculi, the head of caudate nuclei, and a group of brainstem nuclei, have been identified as involved in the organization of the ventral and dorsal attentional networks (Alves et al., 2022).

Despite the established roles of the dorsal and ventral attentional networks in visuospatial attention management, emerging discrepancies regarding their cerebral lateralization reveal a complex picture (Corbetta et al., 2000). Research indicates that visuospatial attention predominantly exhibits rightward lateralization during tasks (Petit et al., 2015; Schuster et al., 2017), yet the extent and direction of this lateralization remain subjects of debate. Notably, the dorsal attentional network is characterized by its bilateral operation in directing attention (Mengotti et al., 2020), with a slight leftward asymmetry at rest contrasted by a rightward asymmetry in its white matter pathways (Alves et al., 2022). Meanwhile, ventral attentional network's bilateral rest activity further complicates our understanding of lateralization within these attentional frameworks (Alves et al., 2022; Mengotti et al., 2020). Finally, visuospatial attentional tasks also engaged executive and controlled processes subtended by prefrontal activations, rarely envisaged under the cerebral lateralization framework. While easily identified as distinct at rest (Gordon et al., 2016; Power et al., 2011; Yan et al., 2023), their naming and spatial topology are inconsistent across studies (Eickhoff et al., 2018; Uddin et al., 2023). Furthermore, task activation during attentional tasks does not respect the boundaries defined by rest, and part of each network can be seen activated conjointly (Corbetta & Shulman, 2011).

Functional lateralization, also known as hemispheric specialization, is defined as the hemisphere-dependent relationship between cognitive, sensory, or motor functions and specific brain structures (Hervé et al., 2013; Tzourio-Mazoyer, 2016). This lateralization indicates the dominance of one hemisphere for certain cognitive functions (Hervé et al., 2013). The lateralization criterion assesses this dominance and enhances the specificity of identifying visuospatial attention areas unique to each

hemisphere (Schuster et al., 2017). Adding a lateralization criterion to the detection of activated areas—defined as the differences between the left and right hemispheres—has previously been used to identify language-specific (Hesling et al., 2019; Labache et al., 2019) and motor areas (Tzourio-Mazoyer et al., 2021). It represents an additional method to increase the specificity in identifying visuospatial attention areas lateralized to the right or left hemisphere. Furthermore, lesion studies have shown that enhancing the specificity for visuospatial attention areas through lateralization criteria helps identify essential areas, those whose impairment leads to spatial neglect (Corbetta & Shulman, 2011), and distinguishes them from non-essential areas revealed by task-induced activation studies.

Here, leveraging a multimodal approach (Hesling et al., 2019; Labache et al., 2019; Tzourio-Mazoyer et al., 2021), we aim to elucidate the anatomo-functional underpinnings and lateralization of visuospatial attentional networks. First, we used a line bisection judgment task in a homogeneous sample of 130 right-handed individuals known for typical language lateralization. We identified significantly involved and asymmetric brain regions related to visuospatial attention, spatial memory, and motor and visual processes required to perform the line bisection judgment task. Second, we explored these identified brain areas' network configuration and topological properties. This exploration is facilitated by applying agglomerative hierarchical clustering to resting-state data, enabling the extraction of distinct networks. Furthermore, we employed graph theory metrics to discern principal hubs integral to visuospatial attention processes. Finally, our study proposed an optimized model of integrated visuospatial attention articulated through a lateralized atlas encompassing 95 well-characterized brain regions, the Atlas for Lateralized visuospatial Attentional Networks (ALANs). This model is a comprehensive framework for future research into the inter-individual variability of visuospatial attentional areas and the mechanisms underlying hemispheric specialization complementarity, enabling reproducible and reliable studies.

2. MATERIAL AND METHODS

2.1. Participants

The study sample consisted of 130 participants from the BIL&GIN (Mazoyer et al., 2016) previously identified as typically brain-organized for language (Labache et al., 2020). The mean age of the sample was 27.3 years ($\sigma = 6.3$; range: 19–53 years; 64 women), and the mean level of education was 16.1 years ($\sigma = 2.1$ years; range: 11–20 years), corresponding to almost 6 years of education

after the French baccalaureate. All participants were right-handed, as assessed with a mean Edinburgh score of +94.2 ($\sigma = 10.3$; Oldfield, 1971). All participants were free of brain abnormalities as assessed by a trained radiologist inspecting their structural T1-MRI scans. All participants gave their informed written consent and received compensation for their participation. The Basse-Normandie Ethics Committee approved the study protocol.

All participants completed a resting-state and two visuospatial task-related fMRI sessions, that is, line bisection judgment and visually guided saccadic eye movements tasks. In the present study, we only report the results of the line bisection judgment.

2.2. The line bisection judgment task

To evaluate the lateralization of spatial attention, we used a line bisection judgment task (Zago et al., 2016). The line bisection judgment task consisted of a 2-sec presentation of a horizontal line bisected by a short vertical line (subtending a visual angle of 1°), followed by a 10-sec delay, during which only a fixation cross appeared on the screen. Participants were asked to decide whether the bisection mark was at the center of the horizontal line or slightly deviated to the left or the right of the center (Fig. 1). They responded by pressing a three-button response pad, with the right index finger for answering "left," the right middle finger for answering "middle," and the right ring finger for answering "right." The horizontal lines were displayed at three different positions along the horizontal axis (-7°, 0°, or +7° of the center of the screen) with three different lengths (6°, 7°, or 9° of visual angle). The bisection mark was deviated by 0.3° on the center's left or right. All parameters were counterbalanced. Thirty-six trials were

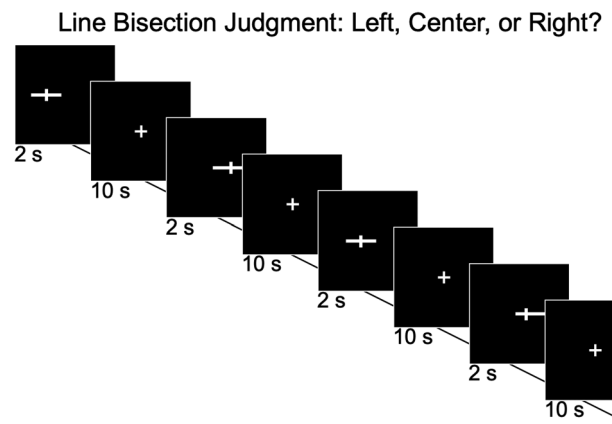


Fig. 1. Line bisection judgment task paradigm. For each trial, the participants were asked to judge if the horizontal line was pre-bisected at its objective middle or if the bisection deviated to the left or right of the midline. A 10-sec fixation delay followed the trial.

presented with an equal number of centered-, leftward-, and right-ward-bisected trials. A 12-sec presentation of a fixation cross preceded and followed the first and last trial, respectively. A practice phase was run outside the scanner.

2.3. Image acquisition

Here, we report the main features of the structural and functional image acquisition previously described by [Mazoyer et al. \(2016\)](#).

2.3.1. Structural image acquisition

Images were acquired using a 3T Philips Intera Achieva scanner (Philips, Eindhoven, The Netherlands). Structural imaging consisted of a high-resolution three-dimensional T1-weighted volume (T1w, sequence parameters: TR: 20 ms; TE: 4.6 ms; flip angle = 10°; inversion time: 800 ms; turbo field echo factor: 65; sense factor: 2; field of view: 256 x 256 x 180 mm³; 1 x 1 x 1 mm³ isotropic voxel size). The line between the anterior and posterior commissures was identified for each participant on a midsagittal section, and the T1-MRI volume was acquired after orienting the brain in this bi-commissural coordinate system. T2*-weighted multi-slice images were also acquired (T2*-weighted fast field echo -T2*-FFE; sequence parameters: TR: 3.500 ms; TE: 35 ms; flip angle = 90°; sense factor: 2; 70 axial slices; 2 x 2 x 2 mm³ isotropic voxel size).

2.3.2. Functional image acquisition

Task-related functional volumes were acquired using a T2*-weighted echo-planar imaging sequence (T2*-EPI; TR: 2 sec; TE: 35 ms; flip angle = 80°; 31 axial slices with a 240 x 240 mm² field of view and 3.75 x 3.75 x 3.75 mm³ isotropic voxel size). The first four volumes of each sequence were discarded to allow for the stabilization of the MR signal.

Resting-state functional volumes were acquired as a single 8-min-long run using the same T2*-EPI sequence (240 volumes) as the fMRI tasks. Before scanning, the participants were instructed to keep their eyes closed to relax, refrain from moving, stay awake, and let their thoughts come and go.

2.4. Image analysis

2.4.1. Functional imaging analysis for task-related and resting-state functional volumes

Both resting state and task-related fMRI data were analyzed using SPM12 software ([www.fil.ion.ucl.ac.uk/spm/](#)) with added in-house MATLAB-based routines. For each

participant, (1) the T2*-FFE volume was rigidly registered to the T1w; (2) the T1w volume was segmented into three brain tissue classes (gray matter, white matter, and cerebrospinal fluid); and (3) the T1w scans were normalized to the BIL&GIN template including 301 volunteers from the BIL&GIN database (aligned to the MNI space) using the SPM12 “normalize” procedure (<http://www.fil.ion.ucl.ac.uk/spm/>) with otherwise default parameters.

Functional data were corrected for slice timing differences and motion. The time courses of the 6 movement-related estimated parameters (3 translations and 3 rotations) were regressed from each voxel T2*-EPI time series. The participant T2*-EPI scans were then rigidly registered to the structural T2*-FFE image. Combining all registration matrices allowed warping the T2*-EPI functional scans from the subject acquisition space to the standard stereotaxic space (2 x 2 x 2 mm³ sampling size) with a single trilinear interpolation.

2.4.2. Specific task-related functional imaging analysis

Global linear modeling (Statistical parametric mapping, SPM12, <http://www.fil.ion.ucl.ac.uk/spm/>) was used to process line bisection judgment-related fMRI data. First, a 6-mm full width at half maximum Gaussian filter was applied to normalized T2*EPI volumes acquired during the line bisection judgment run. The voxel time series were filtered using the SPM software with a 159-sec high pass. Then, for each participant, BOLD variations for each line bisection judgment trial were modeled by a box-car function computed with paradigm timing (2-sec) and convolved with a standard hemodynamic response function (SPM12). The contrast map is estimated by convolving the regressor constructed from the cognitive paradigm's timing with the hemodynamic response function and fitting it within the General Linear Model (GLM) framework. This contrast map defined at the voxel level was subjected to a region of interest analysis. BOLD signal variations were measured in 192 pairs of functionally defined regions of the AICHA atlas ([Joliot et al., 2015](#)) adapted to SPM12, excluding seven region pairs belonging to the orbital and inferior temporal parts of the brain in which signals were reduced due to susceptibility artifacts. For each participant, we computed this contrast map and calculated the right and left region BOLD signal variations for each of the 185 remaining pairs by averaging the contrast BOLD values of all voxels located within the region volume. The AICHA atlas (Atlas of Intrinsic Connectivity of Homotopic Area) was used here since it provides pairs of functionally homotopic regions and is thus well suited to measure functional asymmetries. Due to the brain's inherent Yakovlevian torque, which creates

a global torsion and thus disrupts a perfect point-to-point match between cortical areas that are functionally homotopic (Toga & Thompson, 2003), employing flipped images to compute asymmetries is challenging. This is because the flipped regions do not align precisely with their counterparts in the opposite hemisphere. To address this issue, the AICHA atlas was developed, making it well suited for studying brain hemispheric specialization and lateralization. AICHA circumvents this problem and is thus suited for investigating brain hemispheric specialization and lateralization, allowing the determination of the right and left hemispheric contribution in visuospatial attention processes.

2.4.3. Specific resting-state functional imaging analysis

Time series of BOLD signal variations in white matter and cerebrospinal fluid (individual average time series of voxels that belonged to each tissue class) and temporal linear trends were removed from the rs-fMRI data series using regression analysis. Additionally, rs-fMRI data were bandpass filtered (0.01 Hz–0.1 Hz) using a least-squares linear-phase finite impulse response filter design. For each participant and region, an individual BOLD rs-fMRI time series was computed by averaging the BOLD fMRI time series of all voxels within the region volume.

2.5. Statistical analysis

Statistical analysis was performed using R (R version: 4.2.2; R Core Team, 2021). Data wrangling was performed using the R library *dplyr* (R package version: 1.1.4; Wickham et al., 2023), and data visualization was performed using the R library *ggplot2* (R package version: 3.4.4; Wickham, 2009). Brain visualizations were realized using Surf Ice (NITRC: *Surf Ice: Tool/resource Info*, n.d.), and were made reproducible following guidelines to generate programmatic neuroimaging visualizations (Chopra et al., 2023).

We applied the three-step method previously developed by Labache et al. (2019) to elaborate an atlas for the lateralized visuospatial attention networks. We will briefly outline this method in the subsequent sections.

2.5.1. Identification of the anatomo-functional support of visuospatial attention

To identify the brain asymmetries underpinning the line bisection judgment task, we searched for regions that were significantly both activated and asymmetrical on average among the 130 participants. We conducted a detailed conjunction analysis of the regions that

exhibited significantly positive BOLD signal variations and higher values than their corresponding regions in the opposite hemisphere. A region was selected if it met two criteria: first, its mean t-value was positive, indicating significant activation in the right or left hemisphere at a significance threshold of $p < 3.10^{-4}$, following the Bonferroni correction for multiple comparisons across 185 regions. Second, it demonstrated significant asymmetry at the same significance threshold. The overall significance threshold for these conjunction analyses was set at $p = (3.10^{-4})^2 = 7.10^{-8}$.

2.5.2. Network organization of the lateralized regions

We first computed the intrinsic connectivity matrix for each participant ($n = 130$) to identify resting-state functional connectivity networks among the previously identified regions. The intrinsic connectivity matrix of off-diagonal elements was the Pearson correlation coefficient (r) between the rs-fMRI time series of previously identified region pairs. The connectivity matrices were then Fisher z-transformed using the inverse hyperbolic tangent functions for each individual (R library *psych*; R package version: 2.3.9; William Revelle, 2024) before being averaged and r-transformed with the hyperbolic tangent function.

Second, based on the average connectivity matrix of the sample, we clustered the regions using an agglomerative hierarchical cluster analysis method (Sneath & Sokal, 1973; Ward, 1963). Each region was characterized according to its intrinsic connectivity pattern. Agglomerative hierarchical clustering was performed using Ward's criterion as linkage criteria (Ward, 1963). Before classification, the average connectivity matrix was first transformed into a dissimilarity distance (d) using the following equation: $d = \frac{1-r}{2}$ (Doucet et al., 2011). The optimal number of clusters, determined using the R library *NbClust* (R package version: 1.1.4; Charrad et al., 2014), was found to be five. Based on 17 statistical indices, this method identified the most robust clustering scheme.

Finally, to evaluate the intrinsic inter-network communication, we computed the averaged temporal correlations between networks among the 130 participants. To determine the statistical significance of these correlations, we employed a non-parametric sign test (exact binomial test), with Bonferroni correction for multiple comparisons (10 comparisons), setting the adjusted significance level at $p = 0.005$.

2.5.3. Topological characterization of the networks

We applied the graph theory to analyze intra-network communication across the five identified networks. Notably, we

only included positive correlations in this analysis, as including negative correlations remains a debated topic in the field (Rubinov & Sporns, 2010). Current methods in network theory do not allow for quantifying of the impact of negative functional correlations on the organization of an undirected network, as described here (Power et al., 2010; Rubinov & Sporns, 2010). Incorporating these negative correlations complicates the definition of key concepts, such as the shortest path, due to methods like thresholding, polarity inversion, or adding a constant. These approaches impact the computation of centrality measures, such as betweenness centrality, making the analysis more challenging (Fornito et al., 2016).

We focused on two primary metrics to elucidate the network topology: degree and betweenness centrality. These metrics were instrumental in identifying hub regions, which are pivotal in influencing the overall network structure and flow of information.

Degree centrality (DC) was calculated for each region and each participant within each network as the sum of its positive correlations with other regions within the same network. This measure effectively captures the overall connectedness of a region, highlighting its significance in the network. The degree centrality of the region i for a participant within a given network is then defined by: $DC_i = \sum_{j=1}^N r_{ij}$, where N is the number of regions in the network. On the other hand, betweenness centrality (BC) quantifies the extent to which a region lies on the shortest paths between other regions. The betweenness centrality of the region i for a participant within a given network is then defined by:

$$BC_i = \frac{1}{(N-1)(N-2)} \sum_{h, j, h \neq j, h \neq i, i \neq j} \frac{\rho_{hj}(i)}{\rho_{hj}},$$

where ρ_{hj} is the number of shortest weighted paths (the path that has the lowest sum of correlations between regions) between regions h and j , and $\rho_{hj}(i)$ is the number of shortest weighted paths between regions h and j that pass through region i . $(N-1)(N-2)$ is the number of region pairs that do not include region i . High betweenness centrality values indicate regions that act as essential bridges or intermediaries, facilitating communication across different network segments (Opsahl et al., 2010). Degree and betweenness centrality were computed using the R libraries *igraph* to create and manipulate networks (R package version: 1.5.1; Csardi & Nepusz, 2006; Csárdi et al., 2024), and *qgraph* to compute network measures (R package version: 1.9.8; Epskamp et al., 2012).

We adopted methodologies from Sporns et al. 2007; Opsahl et al., 2010 and van den Heuvel et al. (2010) to determine hub regions. A region was classified as a hub if its degree and betweenness centrality values exceeded the mean and one standard deviation of these measures within the network's regions (Labache et al., 2019). These

identified hubs are crucial for maintaining network connectivity, enabling effective communication, and exerting substantial influence on the dynamics of information flow within the network. The average value of the distribution of degree and betweenness centralities for a given network is defined by: $\overline{DC} = \frac{1}{N} \sum_{i=1}^N \left(\frac{1}{130} \sum_{p=1}^{130} DC_{pi} \right)$, and $\overline{BC} = \frac{1}{N} \sum_{i=1}^N \left(\frac{1}{130} \sum_{p=1}^{130} BC_{pi} \right)$, where N is the number of regions in the network. Similarly, the standard deviation value of the distribution of degree and betweenness centralities for a given network is defined by: $\sigma_{DC} = \sqrt{\frac{1}{N-1} \sum_{i=1}^N \left(\frac{1}{130} \sum_{p=1}^{130} DC_{pi} - \overline{DC} \right)^2}$, and $\sigma_{BC} = \sqrt{\frac{1}{N-1} \sum_{i=1}^N \left(\frac{1}{130} \sum_{p=1}^{130} BC_{pi} - \overline{BC} \right)^2}$.

3. RESULTS

3.1. Identification of the anatomo-functional support of visuospatial attention

We conducted a detailed conjunction analysis to identify the anatomical and functional bases of visuospatial attention.

3.1.1. Right hemisphere

Sixty-six regions met the selection criteria of being significantly activated in the right hemisphere and rightward asymmetrical (Fig. 2). In the occipital lobe, rightward asymmetries were observed in various areas, including the calcarine (CAL3, CAL2), lingual (LING1, LING2, LING4, LING6), and fusiform parts (FUS4, FUS5, FUS6, FUS7), alongside the inferior (O3_2), middle (O2_1, O2_2, O2_3, O2_4), and lateral portions of the occipital gyri (Olat2, Olat4, Olat5), as well as the intraoccipital sulcus (ios).

Within the parietal lobe, clusters of right-sided asymmetries were found in the intraparietal sulcus (ips2, ips3) and the inferior parietal gyrus (P2 and SMG6). On the medial surface, asymmetries were observed in different segments of the precuneus (PRECU1, PRECU7, PRECU8, PRECU9) along the parieto-occipital sulcus (pos1, pos2, pos3, pos5) extending towards the posterior part of the hippocampus (HIPP2) and parahippocampal formation (pHIPP2, pHIPP4, pHIPP5), as well as the anterior pole of the temporal gyrus (poleT2_3).

In the temporal lobe, conjunction of activations and asymmetries were present in the lateral portions of the inferior (T3_3, T3_4, T3_5) and middle (T2_3, T2_4) temporal gyri, as well as in the superior temporal sulcus (STS4 and STS3). Moving to the frontal lobe, regions were identified in the inferior and orbital regions (F3O1,

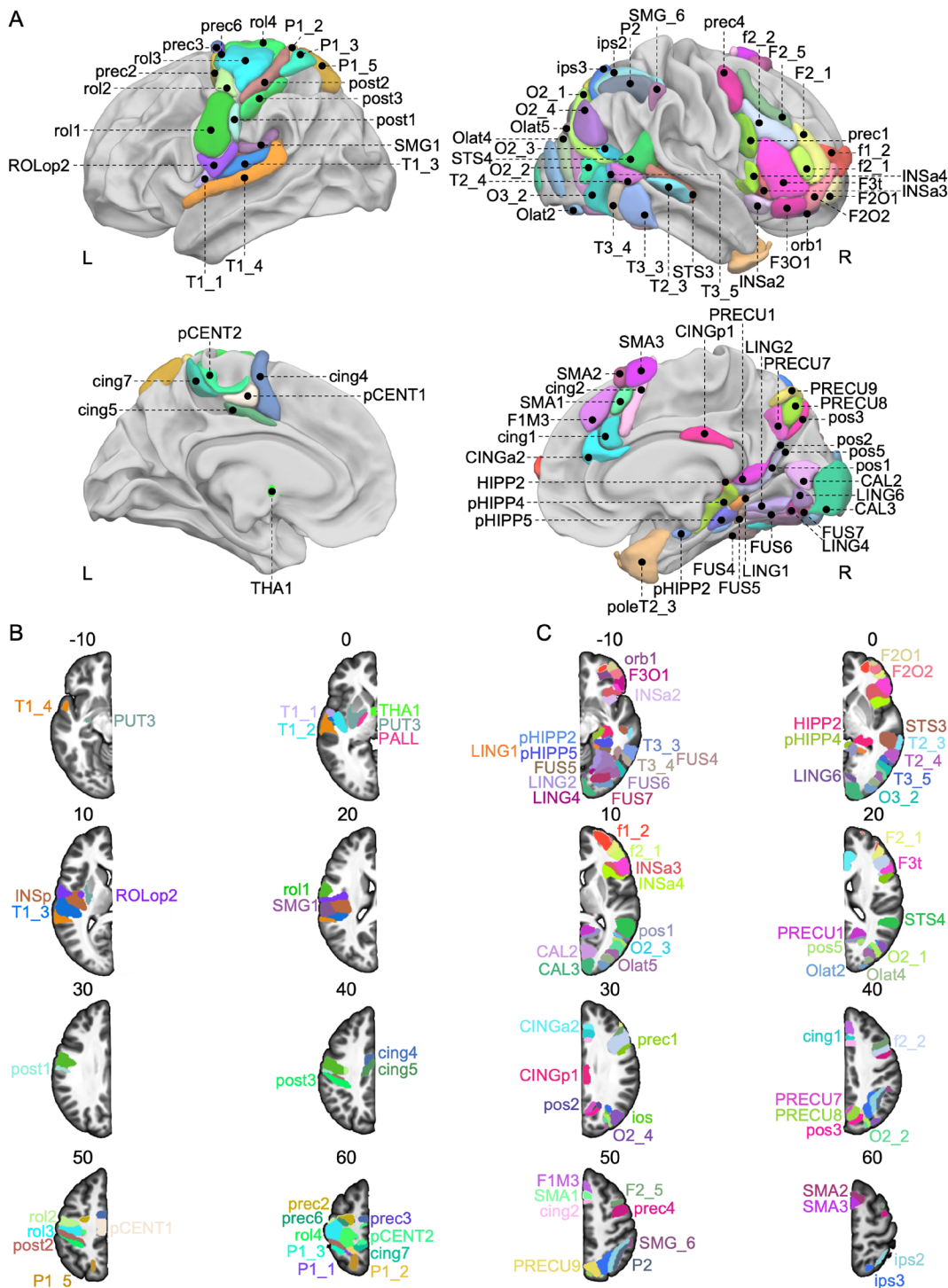


Fig. 2. Locations of the 95 homotopic regions significantly involved in the line bisection judgment task. (A) View of the 29 left and 66 right AICHA regions on the 3D white surface rendering of the BIL&GIN display template in the MNI space with Surf Ice software (<https://www.nitrc.org/projects/surface/>). Top row: Lateral view of the left and right hemispheres, highlighting regions significantly activated and asymmetrical to the left and right, respectively, during the line bisection judgment task. Bottom row: Medial view of the left and right hemispheres, showing similarly activated and asymmetrical regions during the same task. Note that the posterior Insula (INSp), the Putamen (PUT3), the Pallidum (PALL), the Superior Parietal (P1_1), the intraoccipital sulcus (ios), and the Superior Temporal Gyri (T1_2) are not visible in these views. (B) Representation of the 29 regions of the left hemisphere on axial slices of the BIL&GIN display template in the MNI space with MRICroGL software (<https://www.nitrc.org/projects/mricrogl>). (C) Representation of the 66 regions of the right hemisphere on axial slices of the BIL&GIN display template in the MNI space with MRICroGL. The slices' numbers correspond to the z-axis in the MNI space. Correspondences between the abbreviations of the regions and their full names can be found in Table 1. Note that the right Temporal Pole (poleT2_3) is not visible on these axial slices.

F3t, F2O1, F2O2, orb1), extending into the anterior insula (INSA2, INSA3, INSA4). Furthermore, right-brain-dominant asymmetries were observed in the precentral sulcus (prec4 and prec1) and various segments of the middle frontal gyrus (F2_1, F2_5), as well as the inferior and superior frontal sulci (f2_1, f2_2, f1_2). On the medial surface, asymmetries were detected in the supplementary motor area (SMA1, SMA2, SMA3), the median superior frontal gyrus (F1M3), and the anterior and posterior parts of the cingulate gyrus (CINGa2, CINGp1, cing1, cing2).

3.1.2. Left hemisphere

A total of 29 regions met the selection criteria in this study (Fig. 2). Notable asymmetries were observed on the lateral surface, specifically along the Rolandic sulcus (rol1, rol2, rol3, rol4), extending to the precentral sulcus (prec2, prec3, prec6), and the postcentral sulcus (post1, post2, post3) corresponding to the sensorimotor cortex. Leftward asymmetries were also observed in the Rolandic operculum (ROLop2), posterior insula (INSp), and the lower part of the supramarginal gyrus (SMG1). Additionally, subcortical asymmetries favoring the left side were found in the pallidum (PALL), thalamus (THA1), and putamen (PUT3). The superior temporal gyrus (T1_1, T1_2, T1_3, T1_4) and superior parietal gyrus (P1_1, P1_2, P1_3, P1_5) exhibited leftward asymmetry. On the medial face, asymmetry was observed in the posterior sections of the cingulum (cing4, cing5, cing7), as well as two regions in the paracentral lobule (pCENT1, pCENT2).

Correspondences between the abbreviations and the full names of the regions can be found in Table 1.

3.2. Network organization of the lateralized regions

To identify the network organization of the regions, we conducted agglomerative hierarchical clustering on the 95 regions previously identified through conjunction analysis. We then assessed the inter-network communication by examining the temporal correlation across these networks. The significance of these correlations was tested using a non-parametric sign test.

3.2.1. Description of the intrinsic networks

The agglomerative hierarchical clustering analysis revealed five networks from the selected set of 95 asymmetric line bisection judgment-induced regions (Fig. 3; Table 1).

3.2.1.1. Visu network. This network includes 12 regions (Fig. 3, in blue), all located bilaterally in the posterior part of the occipital lobe. We labeled it visu because it

aggregated regions acknowledged as involved in visual processing.

3.2.1.2. Somato-motor network. This network includes most of the cortical regions found in the left hemisphere (Fig. 3, in green). We labeled it somato-motor because it aggregated brain regions involved in the motor and somatosensory aspects of the response production (Tzourio-Mazoyer et al., 2021).

3.2.1.3. Posterior-medial network. This third network encompasses 23 regions (Fig. 3, in orange) located first on the medial surface, namely the dorsal medial parietal regions (precuneus and parieto-occipital sulcus) and the medial temporal regions (posterior part of the hippocampus and the parahippocampus), extending to the anterior fusiform and anterior temporal pole. Secondly, on the lateral surface, it aggregates the posterior part of the intraparietal (ips3) and intra-occipital sulci (ios), extending to the middle occipital gyrus (O2_1, O2_4) to the pole of the middle temporal (poleT2_3) and inferior temporal (T3_3, T3_4) gyri.

3.2.1.4. Temporo-frontal network. This network included 20 regions (Fig. 3, in yellow), 16 being right-lateralized. On the right side, the temporo-frontal network aggregates all the regions located in the inferior and ventral frontal cortex (F3t, F3O1, INSA2, INSA3, INSA4) and the posterior part of the temporal cortex (STS4, STS3, T2_3, T2_4, T3_5) extending to the middle occipital gyrus (O2_3). On the medial wall, this network gathers most of the regions found in the supplementary motor area (SMA2, SMA3) and the anterior cingulate gyrus (cing1, cing2, CINGa2). On the left side, it aggregates the three subcortical regions (PALL, PUT3, and THA1) and the left superior temporal gyrus (T1_4).

3.2.1.5. Parieto-frontal network. This network consists of 15 rightward regions (Fig. 3, in pink), predominantly located in the dorsal and anterior parts of the lateral frontal lobe. These regions include areas along the precentral sulcus (prec1, prec4) and the medial superior frontal cortex (SMA1, F1M3). The network also encompasses the inferior parietal lobe (SMG6, P2) and the intraparietal sulcus (ips_2).

3.2.2. Temporal correlation across networks

The mean rs-fMRI intrinsic connectivity analyses revealed the following correlations between the networks (Fig. 4):

3.2.2.1. Somato-motor and visu networks. There was a positive correlation ($r = 0.37$) between the somato-motor and visu networks. The correlation was statistically significant ($p = 1.10^{-27}$), suggesting a robust association between the two networks.

Table 1. Description of the 95 regions showing joint left activation and left asymmetry (resp. right activation and right asymmetry) during the Line Bisection Judgment task in 130 right-handers.

Network	Abbreviation	Region	Hemisphere	MNI coordinates		
				X (mm)	Y (mm)	Z (mm)
Visu	CAL2	Calcarine Gyrus (2)	Right	10	-78	9
	CAL3	Calcarine Gyrus (3)	Right	11	-94	1
	FUS6	Fusiform Gyrus (6)	Right	29	-62	-9
	FUS7	Fusiform Gyrus (7)	Right	23	-80	-8
	LING2	Lingual Gyrus (2)	Right	21	-60	-6
	LING4	Lingual Gyrus (4)	Right	13	-72	-9
	LING6	Lingual Gyrus (6)	Right	7	-79	-3
	O2_2	Middle Occipital Gyrus (2)	Right	41	-73	12
	O3_2	Inferior Occipital Gyrus (2)	Right	47	-65	-7
	Olat2	lateral occipital Gyrus (2)	Right	28	-89	-2
	Olat4	lateral occipital Gyrus (4)	Right	34	-85	9
	Olat5	lateral occipital Gyrus (5)	Right	36	-76	2
Somato-motor	cing4	cingulate sulcus (4)	Left	-8	-6	57
	cing5	cingulate sulcus (5)	Left	-8	-16	42
	cing7	cingulate sulcus (7)	Left	-9	-41	60
	INSp	Posterior Insula Gyrus	Left	-42	-19	14
	P1_1	Superior Parietal Gyrus (1)	Left	-24	-47	60
	P1_2	Superior Parietal Gyrus (2)	Left	-19	-47	68
	P1_3	Superior Parietal Gyrus (3)	Left	-30	-51	67
	P1_5	Superior Parietal Gyrus (5)	Left	-16	-61	61
	pCENT1	Paracentral Lobule Gyrus (1)	Left	-7	-17	51
	pCENT2	Paracentral Lobule Gyrus (2)	Left	-10	-29	66
	post1	postcentral sulcus (1)	Left	-58	-18	32
	post2	postcentral sulcus (2)	Left	-41	-33	55
	post3	postcentral sulcus (3)	Left	-43	-33	44
	prec2	precentral sulcus (2)	Left	-25	-8	59
	prec3	precentral sulcus (3)	Left	-18	-9	69
	prec6	precentral sulcus (6)	Left	-30	-11	65
	rol1	Rolandic fissure (1)	Left	-54	-8	32
	rol2	Rolandic fissure (2)	Left	-44	-14	51
	rol3	Rolandic fissure (3)	Left	-39	-23	61
	rol4	Rolandic fissure (4)	Left	-23	-29	65
	ROLop2	Rolandic Operculum (2)	Left	-51	-9	14
	SMG1	Supramarginal Gyrus (1)	Left	-54	-30	21
	T1_1	Superior Temporal Gyrus (1)	Left	-55	-1	2
	T1_2	Superior Temporal Gyrus (2)	Left	-45	-11	-2
	T1_3	Superior Temporal Gyrus (3)	Left	-52	-27	11
Posterior-medial	CINGp1	Posterior Cingulate Gyrus (1)	Right	5	-26	29
	FUS4	Fusiform Gyrus (4)	Right	44	-46	-18
	FUS5	Fusiform Gyrus (5)	Right	32	-47	-11
	HIPP2	Hippocampus Gyrus (2)	Right	25	-31	-2
	ios	intraoccipital sulcus (1)	Right	28	-69	33
	ips3	intraparietal sulcus (3)	Right	26	-62	46
	LING1	Lingual Gyrus (1)	Right	20	-44	-4
	O2_1	Middle Occipital Gyrus (1)	Right	36	-74	25
	O2_4	Middle Occipital Gyrus (4)	Right	41	-74	30
	pHIPP2	Parahippocampal Gyrus (2)	Right	29	-25	-19
	pHIPP4	Parahippocampal Gyrus (4)	Right	17	-27	-10
	pHIPP5	Parahippocampal Gyrus (5)	Right	27	-36	-12
	poleT2_3	Middle Tempora Pole Gyrus (3)	Right	26	6	-36
	pos1	parieto-occipital sulcus (1)	Right	13	-54	8
	pos2	parieto-occipital sulcus (2)	Right	16	-61	26
	pos3	parieto-occipital sulcus (3)	Right	14	-73	37
	pos5	parieto-occipital sulcus (5)	Right	21	-66	20
	PRECU1	Precuneus Gyrus (1)	Right	13	-53	14

Table 1. (Continued)

Network	Abbreviation	Region	Hemisphere	MNI coordinates		
				X (mm)	Y (mm)	Z (mm)
Temporo-frontal	PRECU7	Precuneus Gyrus (7)	Right	7	-63	36
	PRECU8	Precuneus Gyrus (8)	Right	11	-68	41
	PRECU9	Precuneus Gyrus (9)	Right	13	-68	50
	T3_3	Inferior Temporal Gyrus (3)	Right	57	-46	-14
	T3_4	Inferior Temporal Gyrus (4)	Right	54	-58	-11
	cing1	cingulate sulcus (1)	Right	7	27	31
	cing2	cingulate sulcus (2)	Right	8	13	47
	CINGa2	Anterior Cingulate Gyrus (2)	Right	7	33	23
	F3O1	Inferior Frontal Gyrus: <i>Pars Orbitalis</i> (1)	Right	44	33	-14
	F3t	Inferior Frontal Gyrus: <i>Pars Triangularis</i> (1)	Right	50	29	5
	INSA2	Anterior Insula Gyrus (2)	Right	35	18	-13
	INSA3	Anterior Insula Gyrus (3)	Right	37	24	-0
	INSA4	Anterior Insula Gyrus (4)	Right	41	15	4
	O2_3	Middle Occipital Gyrus (3)	Right	45	-63	15
	PALL	Pallidum (1)	Left	-19	-8	-1
	PUT3	Putamen (3)	Left	-28	-6	2
	SMA2	Supplementary Motor Area (2)	Right	11	18	63
Parieto-frontal	SMA3	Supplementary Motor Area (3)	Right	6	10	66
	STS3	superior temporal sulcus (3)	Right	53	-32	-0
	STS4	superior temporal sulcus (4)	Right	55	-46	15
	T1_4	Superior Temporal Gyrus (4)	Left	-59	-23	4
	T2_3	Middle Temporal Gyrus (3)	Right	62	-31	-5
	T2_4	Middle Temporal Gyrus (4)	Right	57	-53	3
	T3_5	Inferior Temporal Gyrus (5)	Right	49	-58	4
	THA1	Thalamus (1)	Left	-4	0	1
	f1_2	superior frontal sulcus (2)	Right	28	56	7
	f2_1	inferior frontal sulcus (1)	Right	46	40	10
	f2_2	inferior frontal sulcus (2)	Right	44	19	28
	F1M3	Medial Superior Frontal Gyrus (3)	Right	6	33	45
	F2_1	Middle Frontal Gyrus Gyrus (1)	Right	41	44	13
	F2_5	Middle Frontal Gyrus Gyrus (5)	Right	42	17	41
	F2O1	Middle Orbito-Frontal Gyrus (1)	Right	36	57	-6
	F2O2	Middle Orbito-Frontal Gyrus (2)	Right	40	50	-4
	ips2	intraparietal sulcus (2)	Right	37	-52	48
	orb1	orbital sulcus (1)	Right	26	41	-15
	P2	Inferior Parietal Gyrus (1)	Right	43	-53	48
	prec1	precentral sulcus (1)	Right	50	10	24
	prec4	precentral sulcus (4)	Right	44	1	48
	SMA1	Supplementary Motor Area Gyrus (1)	Right	6	21	49
	SMG6	Supramarginal Gyrus (6)	Right	54	-38	44

The table displays the label of the network to which a region has been clustered, its abbreviation, its full anatomical name, the hemisphere to which it belongs, and the coordinates of its center of mass in MNI space. The number in parentheses in the **Region** column corresponds to the functional subdivision of the region. The names of the regions correspond to the names defined in the AICHA atlas (Joliot et al., 2015).

3.2.2.2. Parieto-frontal and temporo-frontal networks.

The parieto-frontal and temporo-frontal networks also showed a positive correlation ($r = 0.29$). The correlation was statistically significant ($p = 7.10^{-19}$) suggesting a meaningful relationship between the parieto-frontal and temporo-frontal networks.

3.2.2.3. Temporo-frontal and parieto-frontal with somato-motor and visu networks. The temporo-frontal network exhibited positive correlations with both the somato-motor network ($r = 0.25, p = 1.10^{-20}$) and the visu

network ($r = 0.14, p = 3.10^{-10}$), while the parieto-frontal network showed negative correlations with them (somato-motor network, $r = -0.11, p = 2.10^{-5}$; visu network, $r = -0.18, p = 3.10^{-17}$). It reveals a correlated activity of the temporo-frontal network and an anticorrelated activity of the parieto-frontal networks with the somato-motor and visu networks.

3.2.2.4. Posterior-medial with visu and temporo-frontal networks. The posterior-medial network positively correlated with the visu network ($r = 0.11, p = 3.10^{-4}$). However,

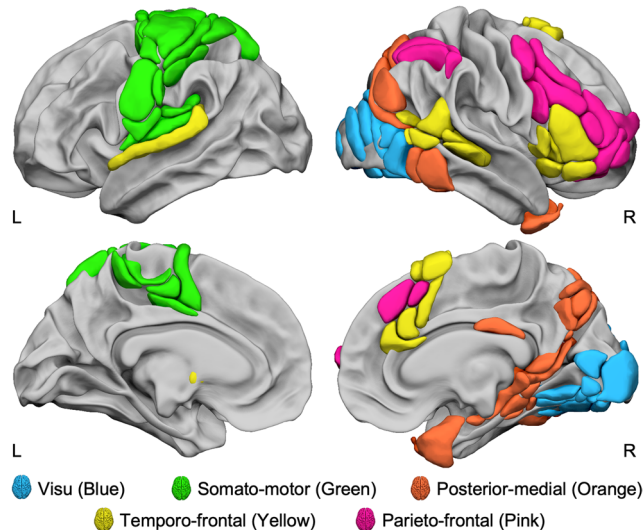


Fig. 3. Lateralized Networks during the Line Bisection Judgment task. Lateral and medial views of the five intrinsic identified networks of the 95 regions asymmetrically involved in the line bisection judgment task, evidenced by the agglomerative hierarchical cluster analysis method. View of 3D white surfaces rendering on the BIL&GIN display template in the MNI space. L: left; R: right.

there was a negative correlation between the posterior-medial and temporo-frontal networks ($r = -0.07, p = 5.10^{-4}$), suggesting potentially different functional characteristics or opposing activity patterns between these networks.

Notably, no significant correlation was found between the posterior-medial network and the somato-motor or parieto-frontal networks ($p > 0.40$ for both), indicating a lack of strong associations between these specific network pairs.

3.3. Topological characterization of the networks

We computed the degree and betweenness centrality to explore the topological organization of the networks and identify crucial hub regions.

Within the **parieto-frontal network**, the hub significance thresholds ($mean + \sigma$) were determined as 6.02 for the Degree Centrality (DC, $mean = 5.07, \sigma = 0.95$, range: [3, 6.18]) and 0.98 for the Betweenness Centrality (BC, $mean = 0.72, \sigma = 0.26$, range: [0.32, 1.35]). Only the inferior frontal sulcus region (f2_2; Fig. 5) met the hub criteria, with a BC value of 1.35 ($CI_{95\%} = [1.06, 1.64]$) and a DC value of 5.99 ($CI_{95\%} = [5.75, 6.22]$).

In the **temporo-frontal network**, hubs were defined by thresholds of 4.74 for DC ($mean = 3.66, \sigma = 1.08$, range: [1.36, 5.08]) and 3.59 for BC ($mean = 2.75, \sigma = 0.84$, range: [1.27, 4.17]). Three regions satisfied the hub definition: F3t (DC = 5.08, $CI_{95\%} = [4.67, 5.49]$; BC = 4.14, $CI_{95\%} = [3.09, 5.19]$), STS4 (DC = 5.04, $CI_{95\%} = [4.65, 5.43]$; BC = 3.62, $CI_{95\%} = [2.07, 4.54]$), and INSa3 (DC = 4.86, $CI_{95\%} = [4.41, 5.31]$; BC = 3.59, $CI_{95\%} = [2.78, 4.40]$) (Fig. 5). INSa3 approached the BC hub threshold but still qualified as a hub.

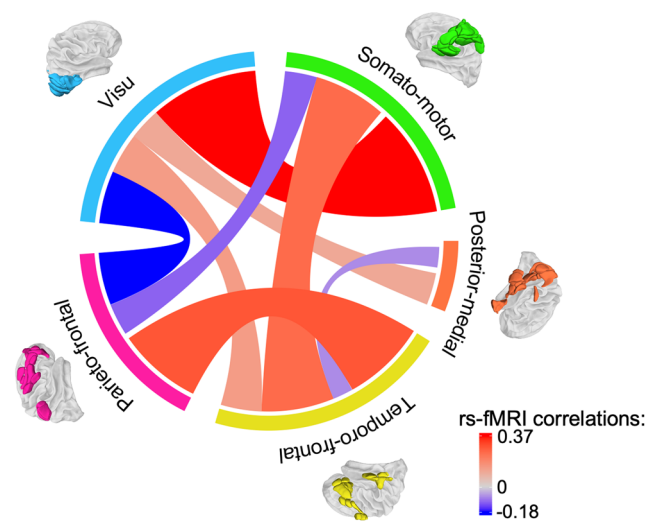


Fig. 4. Average resting-state functional MRI correlation across the five networks. The figure displays the significant average rs-fMRI intrinsic connectivity of each network with each other ($p < 0.005$, Bonferroni correction). Average correlations were computed as the mean of pairwise correlations between regions across the 130 participants. Sectors, representing each of the five networks involved in the line bisection judgment task, were colored as follows: blue for visu, green for somato-motor, orange for posterior-medial, yellow for temporo-frontal, and pink for parieto-frontal networks. Tracks between sectors represented the average correlation between the two linked networks, with the color of the tracks indicating the strength of the correlation: blue for negative correlations and red for positive correlations. The track width is proportional to the strength of the correlation: the larger the correlation, the wider the track width, and vice versa. The scale's minimum and maximum were set to the maximum of the negative and positive correlation distributions.

5.31]; BC = 3.59, $CI_{95\%} = [2.78, 4.40]$) (Fig. 5). INSa3 approached the BC hub threshold but still qualified as a hub.

In the **posterior-medial network**, PRECU1 (DC = 6.11, $CI_{95\%} = [5.90, 6.33]$; BC = 5.30, $CI_{95\%} = [4.58, 6.02]$) and pos2 (DC = 5.82, $CI_{95\%} = [5.58, 6.07]$; BC = 4.59, $CI_{95\%} = [3.97, 5.20]$) were identified as hubs, as their DC and BC values surpassed the set thresholds (DC ≥ 5.41 , $mean = 4.38, \sigma = 1.03$, range: [2.65, 4.38]; BC $\geq 4.55, mean = 3.47, \sigma = 1.08$, range: [1.51, 5.30]) (Fig. 5).

Within the **somato-motor network**, two sensorimotor regions were classified as hubs based on the thresholds of DC ≥ 8.89 ($mean = 7.69, \sigma = 1.20$, range: [4.11, 9.80]) and BC ≥ 1.68 ($mean = 1.36, \sigma = 0.32$, range: [0.61, 1.90]): post2 (DC = 9.27, $CI_{95\%} = [8.86, 9.68]$; BC = 1.68, $CI_{95\%} = [1.40, 1.95]$) and the neighboring cing4 in the medial wall (DC = 9.40, $CI_{95\%} = [9.04, 9.76]$; BC = 1.90, $CI_{95\%} = [1.59, 2.21]$) (Fig. 5).

None of the 12 regions in the **visu network** met the chosen significance thresholds (DC $\geq 5.62, mean = 4.66,$

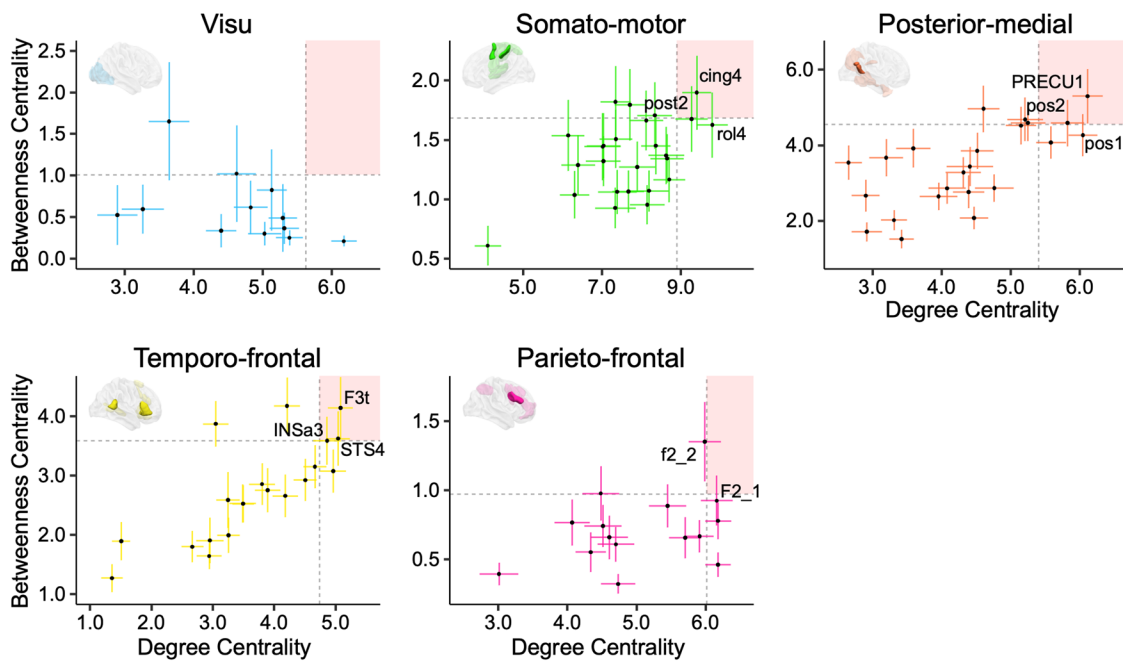


Fig. 5. Identification of hubs. Plots of Degree Centrality (DC) versus Betweenness Centrality (BC) in each of the 5 networks. Bars are 95% confidence intervals for each DC and BC value of each region. The mean plus one standard deviation value of DC and BC defines the quadrant regions located in the right superior quadrant as hubs, which are illustrated on the corresponding hemisphere as solid regions. Abbreviations for the regions can be found in Table 1.

$\sigma = 0.96$, range: [2.90, 6.17]; $BC \geq 1.01$, $mean = 0.60$, $\sigma = 0.41$, range: [0.21, 1.65]), thus not qualifying as hubs (Fig. 5).

4. SUMMARY OF THE RESULTS

In this study, we analyzed the activation and asymmetry of the brain in 130 right-handed participants engaged in a visuospatial attentional line bisection judgment task. Using the AICHA atlas, we identified 95 lateralized regions—66 on the right and 29 on the left. Agglomerative hierarchical clustering based on intrinsic connectivity among these regions yielded five distinct intrinsic networks. These networks were named according to their anatomical locations: visu, somato-motor, posterior-medial, temporo-frontal, and parieto-frontal.

Further analysis revealed notable intrinsic connectivity patterns. Strong positive correlations were observed between the somato-motor and visu networks and between the parieto-frontal and temporo-frontal networks. The temporo-frontal network also showed positive correlations with both the somato-motor and visu networks. Conversely, the parieto-frontal network exhibited negative correlations with the somato-motor and visu networks. Additionally, the posterior-medial network demonstrated positive correlations with the visu network.

Graph metric analysis highlighted key hubs within these networks. Within the temporo-frontal network, the right F3t, right INSa3, and right STS4 regions showed

high degrees of centrality, indicating their significant roles as network hubs. The right-lateralized parieto-frontal network's lateral inferior frontal sulcus region (f2_2) also emerged as a prominent hub. In the posterior-medial network, the PRECU1 and pos2 regions were located in the medial wall in the right precuneus and parieto-occipital sulcus were identified as hubs. Similarly, the pre-supplementary motor area (cing4) and the somato-sensory cortex (post2) regions in the left-lateralized somato-motor network were also recognized as hubs. These hubs are pivotal in facilitating communication and the flow of information within their respective networks.

5. DISCUSSION

Our study identifies lateralized brain networks during a line bisection judgment attention task among a substantial sample of right-handed individuals, showing typical language organization. To investigate brain lateralization, we utilized an fMRI-adapted version of the traditional “paper and pencil” line bisection task. The line bisection task, along with its neuroimaging-adapted variant, has consistently shown its efficacy in inducing both brain and behavioral attentional asymmetries (Benwell et al., 2014; Brooks et al., 2016; Cavézian et al., 2012; Ciçek et al., 2009; Thiebaut de Schotten et al., 2005; Zago, Petit, et al., 2017). Using a multimodal approach, integrating the line bisection judgment task and resting-state acquisition, we identified 95 lateralized regions organized in five networks.

Among these, two key rightward networks—the parieto-frontal and temporo-frontal—demonstrate strong synchronous fMRI signal fluctuations at rest, organized around four core regions: the inferior frontal sulcus, the inferior frontal gyrus (*pars triangularis*), the anterior insula, and the posterior part of the superior temporal sulcus. Together, this work advances our understanding of organizing the anatomo-functional bases of visuospatial attention. It will also enable investigations into brain organization in atypical individuals and assess hemispheric complementarity mechanisms (Johnstone et al., 2020; Tzourio-Mazoyer et al., 2019; Vingerhoets, 2019).

In addition to the typical rightward functional asymmetries in temporoparietal and frontal regions, known to be recruited during visuospatial attentional task-related fMRI studies (Ciçek et al., 2009; Zago et al., 2016; Zago, Petit, et al., 2017), we observed leftward asymmetries in relation to the somato-motor response production. These findings align with the typical brain functional organization, where visuospatial attention exhibits right-hemisphere dominance, and response production demonstrates left-hemisphere dominance in right-handers.

Among these lateralized brain regions recruited during the line bisection judgment task, the intrinsic connectivity analysis distinguished between local networks that clustered visual and somato-motor regions (visu and somato-motor networks) and large-scale networks that clustered temporo-frontal regions (temporo-frontal network), parieto-frontal regions (parieto-frontal network), and posterior medial regions (posterior-medial network). This division aligns with other studies examining global brain intrinsic connectivity (Doucet et al., 2011; Gordon et al., 2016; Yeo et al., 2011). From a methodological perspective, we used hierarchical clustering with Ward's distance to identify and segregate these networks, prioritizing reproducibility and stability in our analytical approach. Unlike methods such as k-means, which may yield spatially cohesive but less reproducible clusters, hierarchical clustering ensures the formation of highly reproducible and well-connected clusters, as evidenced by Thirion et al. (2014). This methodological choice aligns with our aim to produce robust and comparable results that integrate seamlessly with existing lateralized functional atlases (Hesling et al., 2019; Labache et al., 2019) and enhance the reliability of network comparisons across studies.

To contextualize our findings within the existing literature on resting-state networks and facilitate cross-laboratory communication (Uddin et al., 2023), we compared our five-network clustering related to line bisection judgment with the seven-network parcellation proposed by Yan et al. (2023). Following a similar methodology as Labache et al. (2023), this comparative analysis sheds light on the correspondence between our line

bisection judgment-related lateralized networks and established resting-state networks, offering insights into their functional relationships. For each region of the AICHA atlas, we computed a distribution of overlap percentage with all seven canonical networks. Each region was assigned to the network with the greatest overlap (Fig. 6A). As depicted in Figure 6B and C, our five-network clustering approach revealed that the local visual and sensorimotor networks are concordant with those identified by Yan et al. (2023), as evidenced by the significant overlap observed. For example, all regions clustered in the visu network correspond to the Visual canonical network (Fig. 6, in violet), and 72% of the regions in our somato-motor network align with the canonical Som/Motor network (Fig. 6, in blue). Therefore, the overlap between our clustering approach and Yan's parcellation is consistent for the local networks. The parieto-frontal network overlaps with the Control network by 80% and the DorsAttn network by 20%, indicating that the rightward parieto-frontal network groups together brain regions, subtending controlled and goal-oriented attentional processes. The overlap for the two other large-scale temporo-frontal and posterior-medial networks is more scattered, which is consistent with the ongoing challenge in the existing literature to establish a consensus regarding the classification of different large-scale networks across various studies (Uddin et al., 2019; Witt et al., 2021). Each of these networks will be discussed in detail below.

5.1. The parieto-frontal network: A central role in goal-directed orientation and executive control of attention

Our findings demonstrate a significant overlap of the present parieto-frontal network with the frontoparietal Control network (Fig. 6), particularly in regions encompassing the dorsolateral and superior medial prefrontal cortex and the inferior parietal cortex. This overlap underscores the parieto-frontal network's integral role in a variety of executive functions, including cognitive control, attention regulation, and working memory, resonating with descriptions of similar frontoparietal networks in the literature (Uddin et al., 2019; Vincent et al., 2008). The observed lateralization in the parieto-frontal network aligns with studies suggesting hemisphere-specific roles: the right hemisphere's involvement in attentional control and inhibition (Aron et al., 2004; Spagna et al., 2020) and the left hemisphere's dominance in abstraction and hierarchical control, probably associated with the language processes (Nee, 2021). The lateralization of the parieto-frontal network in visuospatial processes highlights its role in interhemispheric balance, being right-lateralized when interacting with attentional regions

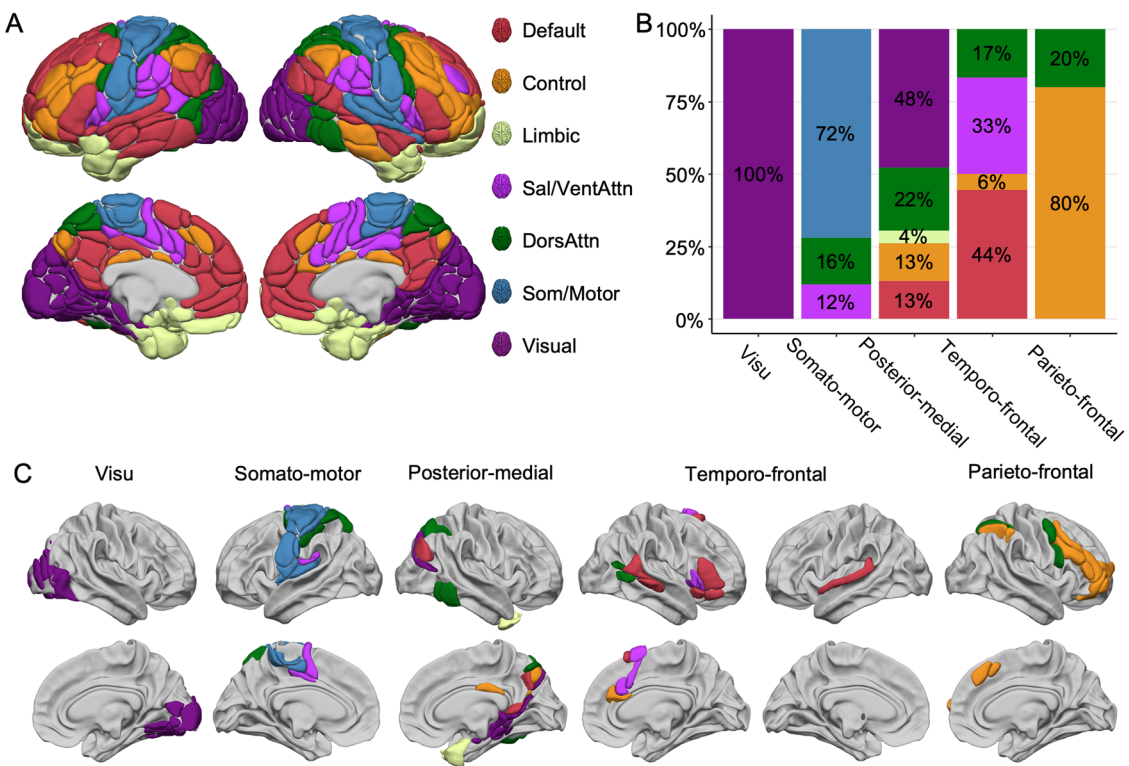


Fig. 6. Comparison between the five ALANs (Atlas of Lateralized visuospatial Attentional Networks) clustered networks and the seven canonical network parcellation by Yeo et al. (2011) as proposed by Yan et al. (2023). (A) The 7-network parcellation is rendered on the AICHA atlas (Joliot et al., 2015). (B) Repartition of the regions of the ALANs five-network parcellation across the seven canonical networks. Color code corresponds to the seven canonical networks. (C) Lateral and medial views of the ALANs networks colored according to Yan et al. (2023) seven-network parcellation. For visu, 100% of the regions pertained to the canonical visual network (violet). For somato-motor, 72% (blue) of the regions were in the Som/Motor network. For the parieto-frontal, 80% of the regions corresponded to the Control network. By contrast, for posterior-medial and temporo-frontal networks, the distribution across the seven canonical networks is more scattered. View of 3D white surfaces rendering on the BIL&GIN display template in the MNI space.

and left-lateralized with language regions, as shown by Wang et al. (2014).

Moreover, the intersection of the parieto-frontal network with the dorsal attention network, particularly in right-hemispheric regions like the precentral sulcus and intraparietal sulcus, further highlights the parieto-frontal network's involvement in attentional orienting, consistent with the task demands of the line bisection judgment task. This finding is bolstered by the graph theory analysis, identifying the inferior frontal sulcus (f2_2) as a hub node, likely mediating between the dorsal orienting and frontoparietal control systems. The role of the right middle frontal cortex (f2_2 and prec_1) as a link between ventral and dorsal networks, as suggested by resting-state functional connectivity studies (Fox et al., 2006), further supports this integrated perspective on attentional control. These results collectively reinforce the concept of lateralized control processes during visuomotor tasks, illuminating the complex interplay of cognitive control and attentional orienting networks in the brain.

5.2. Interhemispheric integration and attentional roles of the temporo-frontal network

In our study, the temporo-frontal network stands out for its unique composition, encompassing both rightward temporal-frontal regions and leftward superior temporal cortex and subcortical nuclei. This bi-hemispheric characteristic positions it as a distinctly interhemispheric network. This aligns with studies on resting-state activity, which often group both left and right temporal regions, underscores the network's involvement in detecting and reorienting attention toward salient stimuli (Menon & Uddin, 2010; Seeley et al., 2007).

Specifically, the inclusion of the left superior temporal gyrus region (T1_4), which exhibits language-related leftward asymmetry (Labache et al., 2019), suggests a broader functional scope for this network than previously recognized. Moreover, the detection of subcortical structures, particularly the thalamus, aligns with recent neuroanatomical models of the ventral (VAN) and dorsal (DAN) Attentional Networks, which emphasize the role

of the pulvinar as a central region modulating information flow processing in attentional processes (Alves et al., 2022).

The right posterior temporal regions identified in our study are parts of the occipitotemporoparietal junction, contributing to a variety of behaviors and functions such as redirecting attention towards task-relevant stimuli within the VAN, self-perception, and social cognition (Corbetta & Shulman, 2002; Saxe & Kanwisher, 2003). Similarly, the right inferior frontal cortex is implicated in diverse cognitive functions, including the inhibition component of the VAN and social cognition. Numerous studies have aimed to delineate the functional subdivisions of these regions using task-based or large-scale network mapping approaches (Geng & Vossel, 2013; Igelström & Graziano, 2017). For example, recent research by Numssen et al. (2021) proposed an anterior/posterior functional specialization of the inferior parietal lobe across attentional, semantic, and social cognitive functions, as well as hemispheres. Additionally, a coactivation-based parcellation of the right inferior frontal gyrus (IFG) revealed a complex functional organization. This organization includes a posterior-to-anterior axis, with action/motor-related functions concentrated in the posterior region and cognition/abstract-related functions in the anterior region. Moreover, a dorsal-to-ventral axis within the posterior IFG corresponds to distinctions between action execution and inhibition, while a similar axis within the anterior IFG delineates reasoning and social cognition functions (Hartwigsen et al., 2019). The rightward regions clustered in the temporo-frontal network likely underlie the bottom-up attentional processes and inhibition required to perform the line bisection judgment task.

Moreover, this complexity is also reflected in the overlap with the 7-networks parcellation (Fig. 6), with 44% of the temporo-frontal network overlapping with the default-mode network (DMN) and 33% with the VAN/Sal network. While the VAN is implicated in reorienting attention to salient stimuli in the environment, particularly when they are unexpected or novel, the Salience network (SN or Sal) is primarily involved in detecting and filtering salient stimuli from the environment that are biologically or emotionally relevant and require immediate attention (Seeley et al., 2007). The SN plays a key role in switching between different brain networks, facilitating the transition from the DMN to the frontoparietal executive network in response to salient stimuli, and includes regions such as the anterior cingulate cortex (ACC), the anterior insula, and parts of the dorsomedial prefrontal cortex (dmPFC). Those two networks share common brain regions, especially the ventral anterior insula. The anterior insula has been also shown to be a key region of the cingulo-opercular network

(CON; Dosenbach et al., 2006). The CON is involved in maintaining task sets, sustaining attention, and cognitive control processes. It includes regions such as the anterior insula, the dorsal anterior cingulate cortex (dACC), the anterior prefrontal cortex, and the operculum. The CON is engaged in tasks requiring sustained attention, response inhibition, and error monitoring. It is associated with maintaining stable cognitive states and regulating attentional processes over time. Our analysis of the temporo-frontal network's asymmetry during the visuospatial task supports its involvement in these complex attentional mechanisms. Notably, the network's hubs in regions like the anterior insula suggest a potential interaction site between the VAN, CON, and SAL networks and also with the DAN (Cazzoli et al., 2021), underscoring its critical role in modulating attentional processes. Finally, the strong positive correlation observed between the parieto-frontal and temporo-frontal networks further emphasizes their collaborative function in attentional control, although further research is needed to fully elucidate the lateralization and functional dynamics of these high-order networks.

5.3. Functional integration and spatial processing in the posterior-medial network

As identified in our study, the posterior-medial network encompasses a range of regions in the right hemisphere, including the posteromedial wall from the precuneus through the medial temporal lobe to the anterior temporal pole. These regions predominantly involve spatial cognition, attention, and memory (Cavanna & Trimble, 2006; Richter et al., 2019; Shulman et al., 2010). Notably, the right precuneus and posterior parietal cortex have been shown to exhibit a rightward bias during visuospatial tasks (Mahayana et al., 2014), suggesting their significant involvement in spatial processing. Compared to the 7-networks parcellation from Yeo et al. (2011), the regions within the posterior-medial network show a diverse overlap across multiple resting-state networks, including visual, dorsal attention, control, and default mode networks. This complex overlap pattern resonates with recent findings that identified intricate hippocampal-parietal circuits and connections to the parietal memory network (Seoane et al., 2022; Zheng et al., 2020), further supporting the involvement of the posterior-medial network in goal-oriented processing and stimulus recognition.

Moreover, connectivity studies, such as those by Zhang and Li (2012), demonstrate that the dorsal precuneus within this network exhibits strong connections with occipital and posterior parietal cortices and areas related to motor execution and visual imagery. This rich

connectivity underscores the network's role in integrating spatial, motor, and visual information. Regarding network correlations, the posterior-medial network showed the lowest overall connectivity, with a positive correlation with the visu network and a slight negative correlation with the temporo-frontal Network, highlighting its distinct functional profile. These findings emphasize the unique positioning of the posterior-medial network in the neural architecture, playing a pivotal role in spatial processing and integrating diverse cognitive functions.

5.4. The local visual and somato-motor networks

In our exploration of local visual (visu) and sensorimotor (somato-motor) networks during the line bisection judgment task, we observed distinct patterns of BOLD asymmetry that align with existing literature on visuospatial attention and sensorimotor processing. Specifically, the visu network demonstrated a pronounced rightward BOLD lateralization, independent of stimulus asymmetry, reflecting the engagement of top-down attentional processes and lateralized modulation of visual cortical regions, consistent with the interactions between the dorsal attention system and the visual occipital cortex (Corbetta & Shulman, 2002; Meehan et al., 2017).

Furthermore, our analysis reveals a robust collaboration between the somato-motor and visu networks, as evidenced by their strong positive temporal correlation in mean intrinsic connectivity. This finding underscores the integrated function of these networks in visuomotor coordination, supporting the hypothesis of their cooperative

role in complex cognitive tasks (Rizzolatti & Matelli, 2003). Additionally, we identified leftward areas overlapping with the dorsal attention network in the left hemisphere (Corbetta & Shulman, 2002; Petit et al., 2009), suggesting a significant role of the left hemisphere in coordinating eye movements in right-handed individuals. This observation, coupled with our findings of leftward asymmetries in regions associated with hand and mouth movements, illustrates the multifaceted nature of the left hemisphere's involvement in visuospatial attention and motor planning in right-handers, underlining its intricate role in integrating eye, hand, and mouth movements during cognitive tasks.

5.5. Evaluating ALANs within the broader spectrum of brain lateralization function

We here compared ALANs to a set of three other atlases we previously developed (Fig. 7). These atlases have all been developed using the same methodology as in the present paper, with all having the purpose of characterizing the anatomo-functional support of lateralized cognitive brain function.

Unlike the visu network, which is exclusively linked to visual processes in the line bisection judgment task, the somato-motor network shows broader cognitive involvement. Specifically, 56% of the leftward somato-motor network was found to be non-specific to visuospatial attention, suggesting its engagement in a wider range of cognitive functions. Specifically, the somato-motor network demonstrated significant overlap with the HAMOTA (HAnd MOtor Area atlas; Tzourio-Mazoyer et al., 2021),

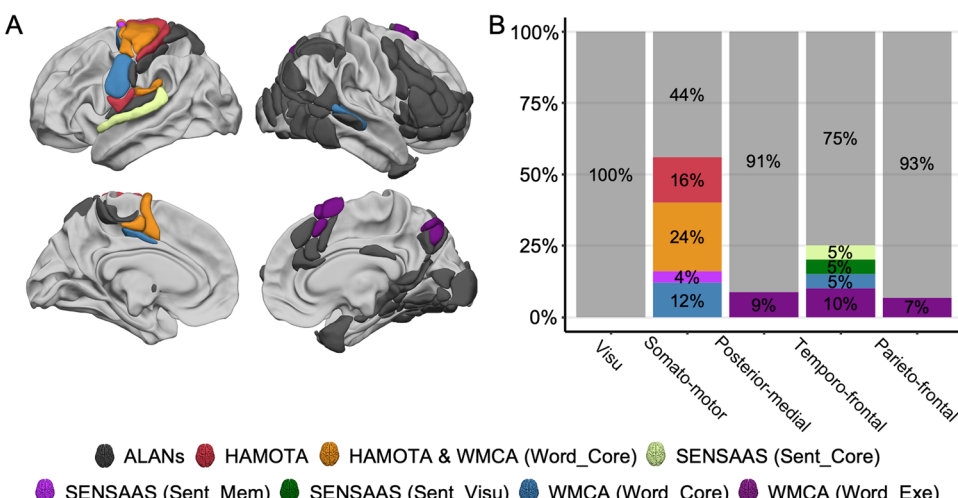


Fig. 7. Comparison between the five ALANs (Atlas of Lateralized visuospatial Attentional Networks) clustered networks and three other functional atlases: HAMOTA: HAnd MOtor Area atlas (Tzourio-Mazoyer et al., 2021), SENSAAS: Sentence Supramodal Areas Atlas (Labache et al., 2019), and WMCA: Word-list Multimodal Cortical Atlas (Hesling et al., 2019). (A) Right and left lateral and medial views of the ALANs atlas. Regions are colored according to the HAMOTA, SENSAAS, and WMCA parcellations. View of 3D white surfaces rendering on the BIL&GIN display template in the MNI space. (B) Repartition of the regions of the ALANs five-network parcellation across HAMOTA, SENSAAS, and WMCA.

WMCA (Word-list Multimodal Cortical Atlas; [Hesling et al., 2019](#)), and SENSAAS (Sentence Supramodal Areas AtlaS; [Labache et al., 2019](#)) atlases ([Fig. 7](#)). This overlap indicates a strong leftward asymmetry in regions associated with somato-motor response production. This asymmetry extends from primary and secondary somatosensory cortices to motor areas ([Fig. 7](#)), highlighting the left hemisphere's dominant role in processing and executing right-hand response production ([Tzourio-Mazoyer et al., 2021](#)) and coordinating subvocal articulation associated with finger selection ([Hesling et al., 2019](#)). Subvocal articulation particularly takes place in the Rolandic fissure (rol1), the only region overlapped by WMCA ([Fig. 7](#); [Hesling et al., 2019](#)) and involved in the mouth, larynx, tongue, jaw, and lip movement. The right precuneus region of the posterior-medial network only overlaps with the executive network of WMCA ([Fig. 7](#)), highlighting its role in mental imagery and/or episodic memory encoding related to the line bisection judgment task ([Cavanna & Trimble, 2006](#)). Concerning the parieto-frontal network, the right supplementary motor area (SMA1, [Fig. 7](#)) is also related to the executive network of WMCA, highlighting its role in evaluating value-based decisions involved in the line bisection judgment task ([So & Stuphorn, 2012](#)). Finally, the temporo-frontal network had 25% of its regions overlapping with either SENSAAS or WMCA ([Fig. 7](#)). Among them, two right supplementary motor areas (SMA2 and SMA3) were related to the executive network of WMCA. The right superior temporal sulcus (STS3), also known as the posterior human voice area ([Pernet et al., 2015](#)), was also found to be a key region in the core network of WMCA. This region is a key area in the interhemispheric communication processes, intertwining between prosodic and phonemic information

([Hesling et al., 2019](#)). Two leftward regions overlapped with SENSAAS: the putamen (PUT_3), supporting executive functions and task monitoring in the processing of multimodal language processing ([Labache et al., 2019](#); [Monchi et al., 2006](#)), and the superior temporal gyrus (T1_4) supporting amodal semantic combinations ([Labache et al., 2019](#); [Price, 2010](#)).

One last significant finding from the comparison of our atlases is depicted in [Figure 8](#), where our analysis unveiled a noteworthy overlap (50%) between regions within the temporo-frontal network and the homotopic counterpart of the core multimodal sentence network ([Labache et al., 2019](#)). Notably, the *pars triangularis* of the inferior frontal gyrus (F3t) and the superior temporal sulcus (STS4), pivotal hubs for the temporo-frontal network, were also hubs for the core network of SENSAAS ([Labache et al., 2019](#)). This indicates a mirror-like organizational similarity between the “ventral” networks of visuospatial attention and language processing, with the peripheral regions of these hubs probably defining the specific processes carried out by each hemisphere. Similarly, the inferior frontal sulcus (f2_2), a hub for the parieto-frontal network, was also a central in the core network of SENSAAS and is on the brink of becoming a hub ([Labache et al., 2019](#)).

The mirrored organizational similarity of the ventral network presents an opportunity to delve into the lateralization of intertwined linguistic and visuospatial processes within specific functions. Sign languages, which exhibit both left and right functional asymmetries ([Emmorey, 2021](#)) and predominantly utilize visual-spatial mechanisms to convey grammatical structure and function ([Courtin et al., 2010](#); [Emmorey et al., 1993](#)), serve as an ideal testing ground for such hypotheses. For example, a recent

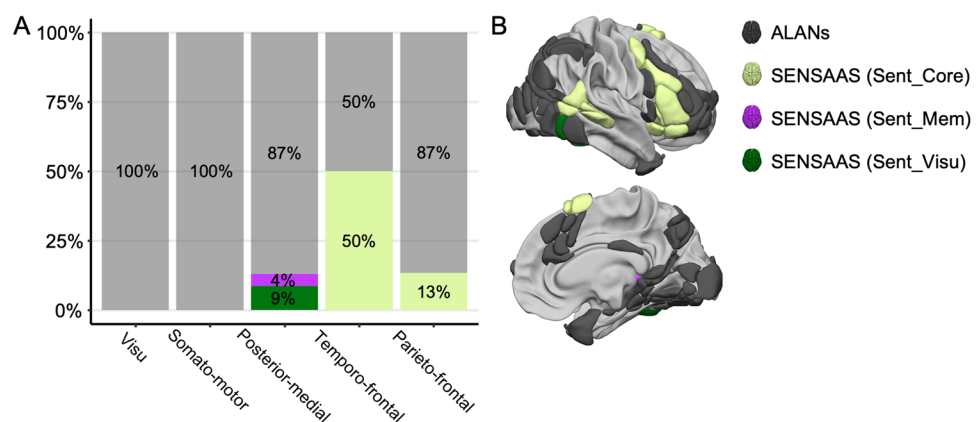


Fig. 8. Comparison between the five ALANs (Atlas of Lateralized visuospatial Attentional Networks) clustered networks and the homotopic version of SENSAAS: Sentence Supramodal Areas Atlas ([Labache et al., 2019](#)). (A) Repartition of the regions of the ALANs five-network parcellation across the homotopic counterpart version of the SENSAAS atlas. (B) Right lateral and medial views of the ALANs atlas. Regions are colored according to the homotopic version of the SENSAAS parcellations. View of 3D white surfaces rendering on the BIL&GIN display template in the MNI space.

meta-analysis of sign language comprehension identified the left posterior inferior frontal gyrus, corresponding to Broca's area, as a supramodal hub responsible for processing linguistic information independently of speech (Trettenbrein et al., 2021).

Moreover, recent findings suggest that as individuals age, language processing regions in the left hemisphere transition from leftward asymmetry to bilateral organization, impacting the symmetry of mnemonic regions as well (Roger et al., 2024). This reorganization indicates a nuanced interplay between language, memory, and visuospatial attention over time that could be specifically studied using the present atlas.

Furthermore, the mirrored organization between language and visuospatial functions observed in typical language-lateralized individuals could offer valuable insights into different language laterality phenotypes (Labache et al., 2020, 2023; Ocklenburg & Güntürkün, 2019; Vingerhoets, 2019; Zago, Hervé, et al., 2017).

All other atlases (including ALANs) of lateralized brain functions mentioned in this section are available to the community here: <https://github.com/loiclabache>.

6. CONCLUSION

Our study elucidates the lateralized brain networks involved in visuospatial attention among right-handed individuals, highlighting the critical roles of the parieto-frontal and temporo-frontal networks. The discovery of significant overlaps with the contralateral sentence network emphasizes a complex interplay between attentional and language processes, shedding light on the brain's functional asymmetry. These insights advance our understanding of cognitive function lateralization and pave the way for future research into atypical brain organization and hemispheric complementarity, with broad implications for both neuroscience and clinical practice. The homotopic Atlas of Lateralized visuospatial Attentional Networks (ALANs) is publicly available as a resource for future studies (Labache, 2024) and can be found here: https://github.com/loiclabache/ALANs_brainAtlas.

DATA AND CODE AVAILABILITY

The data, the code, and the atlas used to produce the results can be found here (Labache, 2024): https://github.com/loiclabache/ALANs_brainAtlas.

AUTHOR CONTRIBUTIONS

Loïc Labache: Conceptualization, Data Curation, Formal Analysis, Investigation, Methodology, Software, Validation, Visualization, Writing—original draft, Writing—review &

editing, Supervision, and Project administration. Laurent Petit: Investigation, Resources, Writing—review & editing, and Funding acquisition. Marc Joliot: Investigation, Resources, Writing—review & editing, and Funding acquisition. Laure Zago: Conceptualization, Validation, Investigation, Resources, Visualization, Writing—original draft, Writing—review & editing, Supervision, Project administration, and Funding acquisition.

DECLARATION OF COMPETING INTEREST

The authors declare no actual or potential conflict of interest.

ACKNOWLEDGEMENTS

We deeply thank Dr. Nathalie Tzourio-Mazoyer for her thoughtful help in discussing the results. The results are part of the BIL&GIN database (Mazoyer et al., 2016).

REFERENCES

- Alves, P. N., Forkel, S. J., Corbetta, M., & Thiebaut de Schotten, M. (2022). The subcortical and neurochemical organization of the ventral and dorsal attention networks. *Communications Biology*, 5(1), 1343. <https://doi.org/10.1038/s42003-022-04281-0>
- Aron, A. R., Robbins, T. W., & Poldrack, R. A. (2004). Inhibition and the right inferior frontal cortex. *Trends in Cognitive Sciences*, 8(4), 170–177. <https://doi.org/10.1016/j.tics.2004.02.010>
- Benwell, C. S. Y., Thut, G., Grant, A., & Harvey, M. (2014). A rightward shift in the visuospatial attention vector with healthy aging. *Frontiers in Aging Neuroscience*, 6, 113. <https://doi.org/10.3389/fnagi.2014.00113>
- Brooks, J. L., Darling, S., Malvaso, C., & Della Sala, S. (2016). Adult developmental trajectories of pseudoneglect in the tactile, visual and auditory modalities and the influence of starting position and stimulus length. *Brain and Cognition*, 103, 12–22. <https://doi.org/10.1016/j.bandc.2015.12.001>
- Cavanna, A. E., & Trimble, M. R. (2006). The precuneus: A review of its functional anatomy and behavioural correlates. *Brain: A Journal of Neurology*, 129(Pt 3), 564–583. <https://doi.org/10.1093/brain/awl004>
- Cavézian, C., Valadao, D., Hurwitz, M., Saoud, M., & Danckert, J. (2012). Finding centre: Ocular and fMRI investigations of bisection and landmark task performance. *Brain Research*, 1437, 89–103. <https://doi.org/10.1016/j.brainres.2011.12.002>
- Cazzoli, D., Kaufmann, B. C., Paladini, R. E., Müri, R. M., Nef, T., & Nyffeler, T. (2021). Anterior insula and inferior frontal gyrus: Where ventral and dorsal visual attention systems meet. *Brain Communications*, 3(1), fcaa220. <https://doi.org/10.1093/braincomms/fcaa220>
- Charrad, M., Ghazzali, N., Boiteau, V., & Niknafs, A. (2014). NbClust: An R Package for determining the relevant number of clusters in a data set. *Journal of Statistical Software*, 61(6), 1–36. <https://doi.org/10.18637/jss.v061.i06>
- Chopra, S., Labache, L., Dhamala, E., Orchard, E. R., & Holmes, A. (2023). A practical guide for generating reproducible and programmatic neuroimaging

- visualizations. *Aperture Neuro*, 3, 1–20. <https://doi.org/10.52294/001c.85104>
- Ciçek, M., Deouell, L. Y., & Knight, R. T. (2009). Brain activity during landmark and line bisection tasks. *Frontiers in Human Neuroscience*, 3, 7. <https://doi.org/10.3389/neuro.09.007.2009>
- Coppens, P., Hungerford, S., Yamaguchi, S., & Yamadori, A. (2002). Crossed aphasia: An analysis of the symptoms, their frequency, and a comparison with left-hemisphere aphasia symptomatology. *Brain and Language*, 83(3), 425–463. [https://doi.org/10.1016/s0093-934x\(02\)00510-2](https://doi.org/10.1016/s0093-934x(02)00510-2)
- Corbetta, M., Kincade, J. M., Ollinger, J. M., McAvoy, M. P., & Shulman, G. L. (2000). Voluntary orienting is dissociated from target detection in human posterior parietal cortex. *Nature Neuroscience*, 3(3), 292–297. <https://doi.org/10.1038/73009>
- Corbetta, M., & Shulman, G. L. (2002). Control of goal-directed and stimulus-driven attention in the brain. *Nature Reviews Neuroscience*, 3(3), 201–215. <https://doi.org/10.1038/nrn755>
- Corbetta, M., & Shulman, G. L. (2011). Spatial neglect and attention networks. *Annual Review of Neuroscience*, 34, 569–599. <https://doi.org/10.1146/annurev-neuro-061010-113731>
- Courtin, C., Hervé, P.-Y., Petit, L., Zago, L., Vigneau, M., Beaucousin, V., Jobard, G., Mazoyer, B., Mellet, E., & Tzourio-Mazoyer, N. (2010). The neural correlates of highly iconic structures and topographic discourse in French Sign Language as observed in six hearing native signers. *Brain and Language*, 114(3), 180–192. <https://doi.org/10.1016/j.bandl.2010.05.003>
- Csardi, G., & Nepusz, T. (2006). The igraph software package for complex network research. *InterJournal Complex Systems*, 1695(5), 1–9. <https://igraph.org/>
- Csárdi, G., Nepusz, T., Müller, K., Horvát, S., Traag, V., Zanini, F., & Noom, D. (2024). *igraph for R: R interface of the igraph library for graph theory and network analysis*. Zenodo. <https://doi.org/10.5281/ZENODO.7682609>
- Dosenbach, N. U. F., Visscher, K. M., Palmer, E. D., Miezin, F. M., Wenger, K. K., Kang, H. C., Burgund, E. D., Grimes, A. L., Schlaggar, B. L., & Petersen, S. E. (2006). A core system for the implementation of task sets. *Neuron*, 50(5), 799–812. <https://doi.org/10.1016/j.neuron.2006.04.031>
- Doucet, G., Naveau, M., Petit, L., Delcroix, N., Zago, L., Crivello, F., Jobard, G., Tzourio-Mazoyer, N., Mazoyer, B., Mellet, E., & Joliot, M. (2011). Brain activity at rest: A multiscale hierarchical functional organization. *Journal of Neurophysiology*, 105(6), 2753–2763. <https://doi.org/10.1152/jn.00895.2010>
- Dronkers, N. F., & Knight, R. T. (1989). Right-sided neglect in a left-hander: Evidence for reversed hemispheric specialization of attention capacity. *Neuropsychologia*, 27(5), 729–735. [https://doi.org/10.1016/0028-3932\(89\)90118-8](https://doi.org/10.1016/0028-3932(89)90118-8)
- Eickhoff, S. B., Yeo, B. T. T., & Genon, S. (2018). Imaging-based parcellations of the human brain. *Nature Reviews Neuroscience*, 19(11), 672–686. <https://doi.org/10.1038/s41583-018-0071-7>
- Emmorey, K. (2021). New perspectives on the neurobiology of sign languages. *Frontiers in Communication*, 6, 748430. <https://doi.org/10.3389/fcomm.2021.748430>
- Emmorey, K., Kosslyn, S. M., & Bellugi, U. (1993). Visual imagery and visual-spatial language: Enhanced imagery abilities in deaf and hearing ASL signers. *Cognition*, 46(2), 139–181. [https://doi.org/10.1016/0010-0277\(93\)90017-p](https://doi.org/10.1016/0010-0277(93)90017-p)
- Epskamp, S., Cramer, A. O. J., Waldorp, L. J., Schmittmann, V. D., & Borsboom, D. (2012). qgraph: Network visualizations of relationships in psychometric data. *Journal of Statistical Software*, 48(4), 1–18. <https://doi.org/10.18637/jss.v048.i04>
- Fornito, A., Zalesky, A., & Bullmore, E. (2016). *Fundamentals of brain network analysis*. Academic Press. <https://doi.org/10.1016/C2012-0-06036-X>
- Fox, M. D., Corbetta, M., Snyder, A. Z., Vincent, J. L., & Raichle, M. E. (2006). Spontaneous neuronal activity distinguishes human dorsal and ventral attention systems. *Proceedings of the National Academy of Sciences of the United States of America*, 103(26), 10046–10051. <https://doi.org/10.1073/pnas.0604187103>
- Francks, C. (2019). In search of the biological roots of typical and atypical human brain asymmetry: Comment on “Phenotypes in hemispheric functional segregation? Perspectives and challenges” by Guy Vingerhoets [Review of *In search of the biological roots of typical and atypical human brain asymmetry: Comment on “Phenotypes in hemispheric functional segregation? Perspectives and challenges” by Guy Vingerhoets*. *Physics of Life Reviews*, 30, 22–24]. <https://doi.org/10.1016/j.plrev.2019.07.004>
- Gazzaniga, M. S. (2000). Cerebral specialization and interhemispheric communication: Does the corpus callosum enable the human condition? *Brain: A Journal of Neurology*, 123(Pt 7), 1293–1326. <https://doi.org/10.1093/brain/123.7.1293>
- Geng, J. J., & Vossel, S. (2013). Re-evaluating the role of TPJ in attentional control: Contextual updating? *Neuroscience and Biobehavioral Reviews*, 37(10 Pt 2), 2608–2620. <https://doi.org/10.1016/j.neubiorev.2013.08.010>
- Gerrits, R. (2022). Variability in hemispheric functional segregation phenotypes: A review and general mechanistic model. *Neuropsychology Review*, 34, 27–40. <https://doi.org/10.1007/s11065-022-09575-y>
- Gordon, E. M., Laumann, T. O., Adeyemo, B., Huckins, J. F., Kelley, W. M., & Petersen, S. E. (2016). Generation and evaluation of a cortical area parcellation from resting-state correlations. *Cerebral Cortex*, 26(1), 288–303. <https://doi.org/10.1093/cercor/bhu239>
- Güntürkün, O., & Ocklenburg, S. (2017). Ontogenesis of lateralization. *Neuron*, 94(2), 249–263. <https://doi.org/10.1016/j.neuron.2017.02.045>
- Hartwigsen, G., Neef, N. E., Camilleri, J. A., Margulies, D. S., & Eickhoff, S. B. (2019). Functional segregation of the right inferior frontal gyrus: Evidence from coactivation-based parcellation. *Cerebral Cortex*, 29(4), 1532–1546. <https://doi.org/10.1093/cercor/bhy049>
- Heger, P., Zheng, W., Rottmann, A., Panfilio, K. A., & Wiehe, T. (2020). The genetic factors of bilaterian evolution. *eLife*, 9, e45530. <https://doi.org/10.7554/eLife.45530>
- Heilman, K. M., Watson, R. T., & Valenstein, E. (1993). Neglect and related disorders. In K. M. Heilman & E. Valenstein (Eds.), *Clinical neuropsychology*, 3rd ed. (pp. 279–336). Oxford University Press.
- Hervé, P.-Y., Zago, L., Petit, L., Mazoyer, B., & Tzourio-Mazoyer, N. (2013). Revisiting human hemispheric specialization with neuroimaging. *Trends in Cognitive Sciences*, 17(2), 69–80. <https://doi.org/10.1016/j.tics.2012.12.004>
- Hesling, I., Labache, L., Joliot, M., & Tzourio-Mazoyer, N. (2019). Large-scale plurimodal networks common to listening to, producing and reading word lists: An fMRI study combining task-induced activation and intrinsic connectivity in 144 right-handers. *Brain Structure & Function*, 224(9), 3075–3094. <https://doi.org/10.1007/s00429-019-01951-4>
- Igelström, K. M., & Graziano, M. S. A. (2017). The inferior parietal lobule and temporoparietal junction: A network

- perspective. *Neuropsychologia*, 105, 70–83. <https://doi.org/10.1016/j.neuropsychologia.2017.01.001>
- Jia, G., Liu, G., & Niu, H. (2021). Hemispheric lateralization of visuospatial attention is independent of language production on right-handers: Evidence from functional near-infrared spectroscopy. *Frontiers in Neurology*, 12, 784821. <https://doi.org/10.3389/fneur.2021.784821>
- Johnstone, L. T., Karlsson, E. M., & Carey, D. P. (2020). The validity and reliability of quantifying hemispheric specialisation using fMRI: Evidence from left and right handers on three different cerebral asymmetries. *Neuropsychologia*, 138, 107331. <https://doi.org/10.1016/j.neuropsychologia.2020.107331>
- Joliot, M., Jobard, G., Naveau, M., Delcroix, N., Petit, L., Zago, L., Crivello, F., Mellet, E., Mazoyer, B., & Tzourio-Mazoyer, N. (2015). AICHA: An atlas of intrinsic connectivity of homotopic areas. *Journal of Neuroscience Methods*, 254, 46–59. <https://doi.org/10.1016/j.jneumeth.2015.07.013>
- Josse, G., & Tzourio-Mazoyer, N. (2004). Hemispheric specialization for language. *Brain Research Reviews*, 44(1), 1–12. <https://doi.org/10.1016/j.brainresrev.2003.10.001>
- Karnath, H.-O., & Rorden, C. (2012). The anatomy of spatial neglect. *Neuropsychologia*, 50(6), 1010–1017. <https://doi.org/10.1016/j.neuropsychologia.2011.06.027>
- Kinsbourne, M. (1970). The cerebral basis of lateral asymmetries in attention. *Acta Psychologica*, 33, 193–201. [https://doi.org/10.1016/0001-6918\(70\)90132-0](https://doi.org/10.1016/0001-6918(70)90132-0)
- Labache, L. (2024). *loiclabache/ALANS_brainAtlas: Labache_2024_ALANS_240214*. Zenodo. <https://doi.org/10.5281/ZENODO.10655105>
- Labache, L., Ge, T., Yeo, B. T. T., & Holmes, A. J. (2023). Language network lateralization is reflected throughout the macroscale functional organization of cortex. *Nature Communications*, 14(1), 3405. <https://doi.org/10.1038/s41467-023-39131-y>
- Labache, L., Joliot, M., Saracco, J., Jobard, G., Hesling, I., Zago, L., Mellet, E., Petit, L., Crivello, F., Mazoyer, B., & Tzourio-Mazoyer, N. (2019). A SENtence Supramodal Areas AtlaS (SENSAAS) based on multiple task-induced activation mapping and graph analysis of intrinsic connectivity in 144 healthy right-handers. *Brain Structure & Function*, 224(2), 859–882. <https://doi.org/10.1007/s00429-018-1810-2>
- Labache, L., Mazoyer, B., Joliot, M., Crivello, F., Hesling, I., & Tzourio-Mazoyer, N. (2020). Typical and atypical language brain organization based on intrinsic connectivity and multitask functional asymmetries. *eLife*, 9, e58722. <https://doi.org/10.7554/eLife.58722>
- Mahayana, I. T., Tcheang, L., Chen, C.-Y., Juan, C.-H., & Muggleton, N. G. (2014). The precuneus and visuospatial attention in near and far space: A transcranial magnetic stimulation study. *Brain Stimulation*, 7(5), 673–679. <https://doi.org/10.1016/j.brs.2014.06.012>
- Mazoyer, B., Mellet, E., Perchey, G., Zago, L., Crivello, F., Jobard, G., Delcroix, N., Vigneau, M., Leroux, G., Petit, L., Joliot, M., & Tzourio-Mazoyer, N. (2016). BiL&GIN: A neuroimaging, cognitive, behavioral, and genetic database for the study of human brain lateralization. *NeuroImage*, 124(Pt B), 1225–1231. <https://doi.org/10.1016/j.neuroimage.2015.02.071>
- Mazoyer, B., Zago, L., Jobard, G., Crivello, F., Joliot, M., Perchey, G., Mellet, E., Petit, L., & Tzourio-Mazoyer, N. (2014). Gaussian mixture modeling of hemispheric lateralization for language in a large sample of healthy individuals balanced for handedness. *PLoS One*, 9(6), e101165. <https://doi.org/10.1371/journal.pone.0101165>
- Meehan, T. P., Bressler, S. L., Tang, W., Astafiev, S. V., Sylvester, C. M., Shulman, G. L., & Corbetta, M. (2017). Top-down cortical interactions in visuospatial attention. *Brain Structure & Function*, 222(7), 3127–3145. <https://doi.org/10.1007/s00429-017-1390-6>
- Mengotti, P., Käsbauer, A.-S., Fink, G. R., & Vossel, S. (2020). Lateralization, functional specialization, and dysfunction of attentional networks. *Cortex; A Journal Devoted to the Study of the Nervous System and Behavior*, 132, 206–222. <https://doi.org/10.1016/j.cortex.2020.08.022>
- Menon, V., & Uddin, L. Q. (2010). Saliency, switching, attention and control: A network model of insula function. *Brain Structure & Function*, 214(5–6), 655–667. <https://doi.org/10.1007/s00429-010-0262-0>
- Mesulam, M. M. (1999). Spatial attention and neglect: Parietal, frontal and cingulate contributions to the mental representation and attentional targeting of salient extrapersonal events. *Philosophical Transactions of the Royal Society of London. Series B, Biological Sciences*, 354(1387), 1325–1346. <https://doi.org/10.1098/rstb.1999.0482>
- Monchi, O., Petrides, M., Strafella, A. P., Worsley, K. J., & Doyon, J. (2006). Functional role of the basal ganglia in the planning and execution of actions. *Annals of Neurology*, 59(2), 257–264. <https://doi.org/10.1002/ana.20742>
- Nee, D. E. (2021). Integrative frontal-parietal dynamics supporting cognitive control. *eLife*, 10, e57244. <https://doi.org/10.7554/eLife.57244>
- NITRC: Surf ice: Tool/resource info. (n.d.). Retrieved March 24, 2022, from <http://www.nitrc.org/projects/surface/>
- Numssen, O., Bzdok, D., & Hartwigsen, G. (2021). Functional specialization within the inferior parietal lobes across cognitive domains. *eLife*, 10, e63591. <https://doi.org/10.7554/eLife.63591>
- Ocklenburg, S., & Güntürkün, O. (2019). Understanding segregated laterality phenotypes needs a comparative perspective on both genotype and enviotype: Comment on “Phenotypes in hemispheric functional segregation? Perspectives and challenges” by Guy Vingerhoets [Review of *Understanding segregated laterality phenotypes needs a comparative perspective on both genotype and enviotype: Comment on “Phenotypes in hemispheric functional segregation? Perspectives and challenges” by Guy Vingerhoets*]. *Physics of Life Reviews*, 30, 25–26. <https://doi.org/10.1016/j.plrev.2019.07.006>
- Oldfield, R. C. (1971). The assessment and analysis of handedness: The Edinburgh inventory. *Neuropsychologia*, 9(1), 97–113. [https://doi.org/10.1016/0028-3932\(71\)90067-4](https://doi.org/10.1016/0028-3932(71)90067-4)
- Opsahl, T., Agneessens, F., & Skvoretz, J. (2010). Node centrality in weighted networks: Generalizing degree and shortest paths. *Social Networks*, 32(3), 245–251. <https://doi.org/10.1016/j.socnet.2010.03.006>
- Pernet, C. R., McAleer, P., Latinus, M., Gorgolewski, K. J., Charest, I., Bestelmeyer, P. E. G., Watson, R. H., Fleming, D., Crabbe, F., Valdes-Sosa, M., & Belin, P. (2015). The human voice areas: Spatial organization and inter-individual variability in temporal and extra-temporal cortices. *NeuroImage*, 119, 164–174. <https://doi.org/10.1016/j.neuroimage.2015.06.050>
- Petersen, S. E., & Posner, M. I. (2012). The attention system of the human brain: 20 years after. *Annual Review of Neuroscience*, 35, 73–89. <https://doi.org/10.1146/annurev-neuro-062111-150525>
- Petit, L., Zago, L., Mellet, E., Jobard, G., Crivello, F., Joliot, M., Mazoyer, B., & Tzourio-Mazoyer, N. (2015). Strong

- rightward lateralization of the dorsal attentional network in left-handers with right sighting-eye: An evolutionary advantage. *Human Brain Mapping*, 36(3), 1151–1164. <https://doi.org/10.1002/hbm.22693>
- Petit, L., Zago, L., Vigneau, M., Andersson, F., Crivello, F., Mazoyer, B., Mellet, E., & Tzourio-Mazoyer, N. (2009). Functional asymmetries revealed in visually guided saccades: An fMRI study. *Journal of Neurophysiology*, 102(5), 2994–3003. <https://doi.org/10.1152/jn.00280.2009>
- Power, J. D., Cohen, A. L., Nelson, S. M., Wig, G. S., Barnes, K. A., Church, J. A., Vogel, A. C., Laumann, T. O., Miezin, F. M., Schlaggar, B. L., & Petersen, S. E. (2011). Functional network organization of the human brain. *Neuron*, 72(4), 665–678. <https://doi.org/10.1016/j.neuron.2011.09.006>
- Power, J. D., Fair, D. A., Schlaggar, B. L., & Petersen, S. E. (2010). The development of human functional brain networks. *Neuron*, 67(5), 735–748. <https://doi.org/10.1016/j.neuron.2010.08.017>
- Price, C. J. (2010). The anatomy of language: A review of 100 fMRI studies published in 2009. *Annals of the New York Academy of Sciences*, 1191, 62–88. <https://doi.org/10.1111/j.1749-6632.2010.05444.x>
- R Core Team (2021). *R: A language and environment for statistical computing*. R Foundation for Statistical Computing. <https://www.R-project.org/>
- Revelle, W. (2024). *psych: Procedures for psychological, psychometric, and personality research*. Northwestern University. <https://CRAN.R-project.org/package=psych>
- Richter, M., Amunts, K., Mohlberg, H., Bludau, S., Eickhoff, S. B., Zilles, K., & Caspers, S. (2019). Cytoarchitectonic segregation of human posterior intraparietal and adjacent parieto-occipital sulcus and its relation to visuomotor and cognitive functions. *Cerebral Cortex*, 29(3), 1305–1327. <https://doi.org/10.1093/cercor/bhy245>
- Rizzolatti, G., & Matelli, M. (2003). Two different streams form the dorsal visual system: Anatomy and functions. *Experimental Brain Research*, 153(2), 146–157. <https://doi.org/10.1007/s00221-003-1588-0>
- Roger, E., Labache, L., Hamlin, N., Kruse, J., Baciu, M., & Doucet, G. E. (2024). When age tips the balance: A dual mechanism affecting hemispheric specialization for language. *bioRxiv: The Preprint Server for Biology*. <https://doi.org/10.1101/2023.12.04.569978>
- Rubinov, M., & Sporns, O. (2010). Complex network measures of brain connectivity: Uses and interpretations. *NeuroImage*, 52(3), 1059–1069. <https://doi.org/10.1016/j.neuroimage.2009.10.003>
- Saxe, R., & Kanwisher, N. (2003). People thinking about thinking people. *The role of the temporo-parietal junction in "theory of mind."* *NeuroImage*, 19(4), 1835–1842. [https://doi.org/10.1016/s1053-8119\(03\)00230-1](https://doi.org/10.1016/s1053-8119(03)00230-1)
- Schuster, V., Herholz, P., Zimmermann, K. M., Westermann, S., Frässle, S., & Jansen, A. (2017). Comparison of fMRI paradigms assessing visuospatial processing: Robustness and reproducibility. *PLoS One*, 12(10), e0186344. <https://doi.org/10.1371/journal.pone.0186344>
- Seeley, W. W., Menon, V., Schatzberg, A. F., Keller, J., Glover, G. H., Kenna, H., Reiss, A. L., & Greicius, M. D. (2007). Dissociable intrinsic connectivity networks for salience processing and executive control. *The Journal of Neuroscience: The Official Journal of the Society for Neuroscience*, 27(9), 2349–2356. <https://doi.org/10.1523/jneurosci.5587-06.2007>
- Seoane, S., Modroño, C., González-Mora, J. L., & Janssen, N. (2022). Medial temporal lobe contributions to resting-state networks. *Brain Structure & Function*, 227(3), 995–1012. <https://doi.org/10.1007/s00429-021-02442-1>
- Shulman, G. L., Pope, D. L. W., Astafiev, S. V., McAvoy, M. P., Snyder, A. Z., & Corbetta, M. (2010). Right hemisphere dominance during spatial selective attention and target detection occurs outside the dorsal frontoparietal network. *The Journal of Neuroscience: The Official Journal of the Society for Neuroscience*, 30(10), 3640–3651. <https://doi.org/10.1523/jneurosci.4085-09.2010>
- Sneath, P. H., & Sokal, R. R. (1973). *Numerical taxonomy. The principles and practice of numerical classification (a series of books in biology)* (Vol. 573). WF Freeman and Co.
- So, N., & Stuphorn, V. (2012). Supplementary eye field encodes reward prediction error. *The Journal of Neuroscience: The Official Journal of the Society for Neuroscience*, 32(9), 2950–2963. <https://doi.org/10.1523/jneurosci.4419-11.2012>
- Spagna, A., Kim, T. H., Wu, T., & Fan, J. (2020). Right hemisphere superiority for executive control of attention. *Cortex: A Journal Devoted to the Study of the Nervous System and Behavior*, 122, 263–276. <https://doi.org/10.1016/j.cortex.2018.12.012>
- Sporns, O., Honey, C. J., & Kötter, R. (2007). Identification and classification of hubs in brain networks. *PLoS One*, 2(10), e1049. <https://doi.org/10.1371/journal.pone.0001049>
- Suchan, J., & Karnath, H.-O. (2011). Spatial orienting by left hemisphere language areas: A relict from the past? *Brain: A Journal of Neurology*, 134(Pt 10), 3059–3070. <https://doi.org/10.1093/brain/awr120>
- Thiebaut de Schotten, M., Friedrich, P., & Forkel, S. J. (2019). One size fits all does not apply to brain lateralisation: Comment on “Phenotypes in hemispheric functional segregation? Perspectives and challenges” by Guy Vingerhoets [Review of One size fits all does not apply to brain lateralisation: Comment on “Phenotypes in hemispheric functional segregation? Perspectives and challenges” by Guy Vingerhoets]. *Physics of Life Reviews*, 30, 30–33. <https://doi.org/10.1016/j.plrev.2019.07.007>
- Thiebaut de Schotten, M., Urbanski, M., Duffau, H., Volle, E., Lévy, R., Dubois, B., & Bartolomeo, P. (2005). Direct evidence for a parietal-frontal pathway subserving spatial awareness in humans. *Science*, 309(5744), 2226–2228. <https://doi.org/10.1126/science.1116251>
- Thirion, B., Varoquaux, G., Dohmatob, E., & Poline, J.-B. (2014). Which fMRI clustering gives good brain parcellations? *Frontiers in Neuroscience*, 8, 167. <https://doi.org/10.3389/fnins.2014.00167>
- Toga, A. W., & Thompson, P. M. (2003). Mapping brain asymmetry. *Nature Reviews Neuroscience*, 4(1), 37–48. <https://doi.org/10.1038/nrn1009>
- Trittenbrein, P. C., Papitto, G., Friederici, A. D., & Zaccarella, E. (2021). Functional neuroanatomy of language without speech: An ALE meta-analysis of sign language. *Human Brain Mapping*, 42(3), 699–712. <https://doi.org/10.1002/hbm.25254>
- Tzourio-Mazoyer, N. (2016). Intra- and Inter-hemispheric connectivity supporting hemispheric specialization. In H. Kennedy, D. C. Van Essen, & Y. Christen (Eds.), *Micro-, meso- and macro-connectomics of the brain*. Springer. https://doi.org/10.1007/978-3-319-27777-6_9
- Tzourio-Mazoyer, N., Labache, L., Zago, L., Hesling, I., & Mazoyer, B. (2021). Neural support of manual preference revealed by BOLD variations during right and left finger-tapping in a sample of 287 healthy adults balanced for handedness. *Laterality*, 26(4), 398–420. <https://doi.org/10.1080/1357650x.2020.1862142>
- Tzourio-Mazoyer, N., Zago, L., Cochet, H., & Crivello, F. (2020). Development of handedness, anatomical and

- functional brain lateralization. *Handbook of Clinical Neurology*, 173, 99–105. <https://doi.org/10.1016/b978-0-444-64150-2.00011-3>
- Tzourio-Mazoyer, N., Zago, L., & Mazoyer, B. (2019). What can we learn from healthy atypical individuals on the segregation of complementary functions?: Comment on “Phenotypes in hemispheric functional segregation? Perspectives and challenges” by Guy Vingerhoets [Review of *What can we learn from healthy atypical individuals on the segregation of complementary functions?: Comment on “Phenotypes in hemispheric functional segregation? Perspectives and challenges” by Guy Vingerhoets*]. *Physics of Life Reviews*, 30, 34–37. <https://doi.org/10.1016/j.plrev.2019.09.003>
- Tzourio, N., Crivello, F., Mellet, E., Nkanga-Ngila, B., & Mazoyer, B. (1998). Functional anatomy of dominance for speech comprehension in left handers vs right handers. *NeuroImage*, 8(1), 1–16. <https://doi.org/10.1006/nimg.1998.0343>
- Uddin, L. Q., Betzel, R. F., Cohen, J. R., Damoiseaux, J. S., De Brigard, F., Eickhoff, S. B., Fornito, A., Gratton, C., Gordon, E. M., Laird, A. R., Larson-Prior, L., McIntosh, A. R., Nickerson, L. D., Pessoa, L., Pinho, A. L., Poldrack, R. A., Razi, A., Sadaghiani, S., Shine, J. M., ... Spreng, R. N. (2023). Controversies and progress on standardization of large-scale brain network nomenclature. *Network Neuroscience (Cambridge, Mass.)*, 7(3), 864–905. https://doi.org/10.1162/netn_a_00323
- Uddin, L. Q., Yeo, B. T. T., & Spreng, R. N. (2019). Towards a universal taxonomy of macro-scale functional human brain networks. *Brain Topography*, 32(6), 926–942. <https://doi.org/10.1007/s10548-019-00744-6>
- van den Heuvel, M. P., Mandl, R. C. W., Stam, C. J., Kahn, R. S., & Hulshoff Pol, H. E. (2010). Aberrant frontal and temporal complex network structure in schizophrenia: A graph theoretical analysis. *The Journal of Neuroscience: The Official Journal of the Society for Neuroscience*, 30(47), 15915–15926. <https://doi.org/10.1523/jneurosci.2874-10.2010>
- Vincent, J. L., Kahn, I., Snyder, A. Z., Raichle, M. E., & Buckner, R. L. (2008). Evidence for a frontoparietal control system revealed by intrinsic functional connectivity. *Journal of Neurophysiology*, 100(6), 3328–3342. <https://doi.org/10.1152/jn.90355.2008>
- Vingerhoets, G. (2019). Phenotypes in hemispheric functional segregation? Perspectives and challenges. *Physics of Life Reviews*, 30, 1–18. <https://doi.org/10.1016/j.plrev.2019.06.002>
- Wang, D., Buckner, R. L., & Liu, H. (2014). Functional specialization in the human brain estimated by intrinsic hemispheric interaction. *The Journal of Neuroscience: The Official Journal of the Society for Neuroscience*, 34(37), 12341–12352. <https://doi.org/10.1523/jneurosci.0787-14.2014>
- Ward, J. H., Jr. (1963). Hierarchical grouping to optimize an objective function. *Journal of the American Statistical Association*, 58(301), 236–244. <https://doi.org/10.1080/01621459.1963.10500845>
- Wickham, H. (2009). *Ggplot2: Elegant graphics for data analysis* (1st ed.). Springer. <https://doi.org/10.1007/978-0-387-98141-3>
- Wickham, H., François, R., Henry, Y. L., Müller, K., & Vaughan, D. (2023). *dplyr: A Grammar of Data Manipulation* (Version 1.0.10). <https://dplyr.tidyverse.org/>; <https://github.com/tidyverse/dplyr>
- Witt, S. T., van Ettinger-Veenstra, H., Salo, T., Riedel, M. C., & Laird, A. R. (2021). What executive function network is that? An image-based meta-analysis of network labels. *Brain Topography*, 34(5), 598–607. <https://doi.org/10.1007/s10548-021-00847-z>
- Yan, X., Kong, R., Xue, A., Yang, Q., Orban, C., An, L., Holmes, A. J., Qian, X., Chen, J., Zuo, X.-N., Zhou, J. H., Fortier, M. V., Tan, A. P., Gluckman, P., Chong, Y. S., Meaney, M. J., Bzdok, D., Eickhoff, S. B., & Yeo, B. T. T. (2023). Homotopic local-global parcellation of the human cerebral cortex from resting-state functional connectivity. *NeuroImage*, 273, 120010. <https://doi.org/10.1016/j.neuroimage.2023.120010>
- Yeo, B. T. T., & Eickhoff, S. B. (2016). Systems neuroscience: A modern map of the human cerebral cortex [Review of *Systems neuroscience: A modern map of the human cerebral cortex*]. *Nature*, 536(7615), 152–154. <https://doi.org/10.1038/nature18914>
- Yeo, B. T. T., Krienen, F. M., Sepulcre, J., Sabuncu, M. R., Lashkari, D., Hollinshead, M., Roffman, J. L., Smoller, J. W., Zöllei, L., Polimeni, J. R., Fischl, B., Liu, H., & Buckner, R. L. (2011). The organization of the human cerebral cortex estimated by intrinsic functional connectivity. *Journal of Neurophysiology*, 106(3), 1125–1165. <https://doi.org/10.1152/jn.00338.2011>
- Zago, L., Hervé, P.-Y., Genuer, R., Laurent, A., Mazoyer, B., Tzourio-Mazoyer, N., & Joliot, M. (2017). Predicting hemispheric dominance for language production in healthy individuals using support vector machine. *Human Brain Mapping*, 38(12), 5871–5889. <https://doi.org/10.1002/hbm.23770>
- Zago, L., Petit, L., Jobard, G., Hay, J., Mazoyer, B., Tzourio-Mazoyer, N., Karnath, H.-O., & Mellet, E. (2017). Pseudoneglect in line bisection judgement is associated with a modulation of right hemispheric spatial attention dominance in right-handers. *Neuropsychologia*, 94, 75–83. <https://doi.org/10.1016/j.neuropsychologia.2016.11.024>
- Zago, L., Petit, L., Mellet, E., Jobard, G., Crivello, F., Joliot, M., Mazoyer, B., & Tzourio-Mazoyer, N. (2016). The association between hemispheric specialization for language production and for spatial attention depends on left-hand preference strength. *Neuropsychologia*, 93(Pt B), 394–406. <https://doi.org/10.1016/j.neuropsychologia.2015.11.018>
- Zhang, S., & Li, C.-S. R. (2012). Functional connectivity mapping of the human precuneus by resting state fMRI. *NeuroImage*, 59(4), 3548–3562. <https://doi.org/10.1016/j.neuroimage.2011.11.023>
- Zheng, A., Montez, D. F., Marek, S., Gilmore, A. W., Newbold, D. J., Laumann, T. O., Kay, B. P., Seider, N. A., Van, A. N., Hampton, J. M., Alexopoulos, D., Schlaggar, B. L., Sylvester, C. M., Greene, D. J., Shimony, J. S., Nelson, S. M., Wig, G. S., Gratton, C., McDermott, K. B., ... Dosenbach, N. U. F. (2020). Parallel hippocampal-parietal circuits for self- and goal-oriented processing. *bioRxiv: The Preprint Server for Biology*. <https://doi.org/10.1101/2020.12.01.395210>